NUREG-0724

Problems in Modeling of Small Break LOCA

Manuscript Completed: September 1980
Date Published: October 1980

N. Zuber

Division of Reactor Safety Research
Office of Nuclear Regulatory Research
U.S. Nuclear Regulatory Commission
Washington, D.C. 20555

Abstract

This report considers two-phase flow phenomena which may occur in horizontal pipes during a small break LOCA. Specifically, it deals with:

1. Two-phase flow regime transitions

2. Liquid entrainment in break flow

3. Vapor pull-through

4. Counter-current flow limitation (CCFL).

The first three processes influence the mass flow rate through the break, whereas the fourth one imposes a limit on the liquid flow from the steam generator through the hot leg back into the core.

The report presents some of the results and correlations available in the literature which can be used to estimate conditions in a duct or at a break, that can lead to a two-phase mixture reaching the break. These correlations are then applied to a hot leg of a PWR, LOFT and Semiscale for quantitative estimates. Secondly, the report deals with rules that scale the four processes noted above. These rules are then applied again, to a hot leg of a PWR, LOFT and Semiscale, to determine the scale distortion in the latter two facilities.

Calculations indicate that conditions which may lead to the occurrence of these four processes in a PWR, are bracketed by those scaled to LOFT and to Semiscale.

It should be stressed that data and correlations available in the literature, which are summarized and used in this report, often do not correspond exactly to conditions that one could expect in a PWR. Consequently, the results presented in this report must not be used for definitive quantitative statements. However, they may be useful for making estimates as well as for guiding experiments and interpreting their results.

Table of Contents

Acknowledgements

The writer is indebted to Drs. P. Andersen, I. Catton, A. Dukler, S. Fabic and A. Olson for stimulating discussions, as well as for information they made available during the preparation of this report.

Nomenclature

[M,L,T system of units]

A_c = cross-sectional area, $[L^2]$

C_D = drag coefficient, [-]

d = break diameter, [L]

D = pipe diameter, [L]

g = gravitational acceleration, $[LT^{-2}]$

F = Froude number [-]

h = enthalpy per unit mass, $[L^2T^{-2}]$

H = height, [L]

j = superficial velocity, $[LT^{-1}]$

K = friction factor, [-]

ℓ = length, [L]

L = distance from interface to break (see Figure A-1) [L]

P = pressure $[ML^{-1}T^{-2}]$

q = heat flux $[MT^{-3}]$

Q = volumetric flow rate, $[L^3T^{-1}]$

t = time, [T]

v = velocity in the pipe $[LT^{-1}]$

V = velocity at the break $[LT^{-1}]$

$\mathcal{V} = \ell A_c$ = volume $[L^3]$

W = mass flow rate $[MT^{-1}]$

Greek Letters

α = void fraction [-]

β = angle defined in Figure A-1

Γ = circulation $[L^2T^{-1}]$

Δ = distortion [-]

ν = kinematic viscosity [L^2T^{-1}]

ρ = density [ML^{-3}]

$\Delta\rho = \rho_l - \rho_g$ [ML^{-3}]

θ = angle defined in Figure A-1

τ = wall stress [$ML^{-1}T^{-2}$]

ϕ = power [ML^2T^{-3}]

ζ = perimeter defined in Figure A-1

Subscripts

g = gas

i = interface

l = liquid

m = model

p = prototype

w = wall

1. Introduction

This report considers two-phase flow phenomena which may occur in horizontal pipes during a small break LOCA. Specifically, it deals with:

1. Two-phase flow regime transitions
2. Liquid entrainment in break flow
3. Vapor pull-through
4. Counter-current flow limitation (CCFL).

The first three processes influence the mass flow rate through the break, whereas the fourth one imposes a limit on the liquid flow from the steam generator through the hot leg back into the core.

There are two reasons for considering these phenomena. One is generated by the need to perform analyses of small break LOCA the other by the requirement to conduct appropriate experiments.

From the point of view of analysis, that is of code calculations, it is necessary to know the composition of the fluid reaching the break. Specifically, one needs to know whether it consists of a single phase (gas or liquid) or of a two phase mixture. Furthermore, one would like to know what criteria and/or experimental data are available which could be used to estimate this state of the fluid.

From the experimental point of view, it is necessary to know what are the scaling rules which describe the phenomena noted above. Specifically, do these rules obey the power to volume scaling of LOFT, Ref 1, and of Semiscale? If not, what is the scale distortion and, if desirable, what changes and/or compromises can be made?

These questions are relevant because according to the power to volume scaling (see Appendix B or Ref 1 through Ref 3), velocities scale as

$$\frac{v_m}{v_p} = \frac{\ell_m}{\ell_p} \qquad 1\text{-}1$$

where ℓ_m and ℓ_p are the length of the corresponding ducts in the model and in the plant respectively. Furthermore, power to volume is a time preserving scale, that is, it satisfies the requirement of isochronicity:

$$\frac{t_m}{t_p} = 1 \qquad 1\text{-}2$$

However, for gravity dominated, free surface flows which could be expected to occur in horizontal ducts, it is well known (see for example Ref 4), that velocities and time scale according to

$$\frac{v_m}{v_p} = \frac{H_{1m}}{H_{1p}} \qquad 1\text{-}3$$

and

$$\frac{t_m}{t_p} = \frac{\ell_m}{\ell_p} \sqrt{\frac{H_{1p}}{H_{1m}}} \qquad 1\text{-}4$$

where, H_{lm} and H_{lp} are the depths of the horizontally flowing liquid in the model and in the prototype respectively. The notation, that is nomenclature used in this report is illustrated in Figure A-1 of Appendix A.

This report is addressed to both aspects of problem, that is, to analysis and experiments. First, the report presents some of the results and correlations available in the literature which can be used to estimate conditions in a duct or at a break, that can lead to a two-phase mixture reaching the break. These correlations are then applied to a hot leg of a PWR, LOFT and Semiscale for quantitative estimates. Secondly, the report deals with rules that scale the four processes noted above. These rules are then applied again, to a hot leg of a PWR, LOFT and Semiscale, to determine the scale distortion in the latter two facilities.

It should be stressed that data and correlations available in the literature, which are summarized and used in this report, often do not correspond exactly to conditions that one could expect in a PWR.* Consequently, the results presented in this report must not be used for definitive quantitative statements. However, they can be used for making estimates as well as for guiding experiments and interpreting their results.

---

* Such cases and resulting restrictions are noted in the discussion of particular correlations and/or data.

2. Two-Phase Flow Regime Transitions

2.1 Scaling

There are several two-phase flow regime maps which can be used to estimate flow regime transitions in horizontal pipes. In what follows, we shall use that proposed by Dukler and Taitel, Ref 5, which is shown in Figure 2-1. It can be seen that in the separated flow regime, a necessary (but not sufficient) condition for single phase flow to reach the break, is for the break to be located above or below the horizontal interface. Consequently, one of the processes which will result in a two-phase mixture reaching the break can be associated with flow regime transition, that is, from separated to slug or to annular-dispersed flow.

It can be seen from Figure 2-1, that flow regime boundaries depend on the dimensionless liquid depth: H_l/D, and on the Froude number for the vapor given by:

$$F = \frac{j_g \sqrt{\rho_g}}{\sqrt{g \Delta \rho D}} \qquad 2\text{-}1$$

that is, the regime transitions are specified by

$$F = \frac{j_g \sqrt{\rho_g}}{\sqrt{g \Delta \rho D}} = f\left(\frac{H_l}{D}\right) \qquad 2\text{-}2$$

It is shown in Appendix A, that in separated flow, the requirement of geometric similarity implies equality of void fractions:

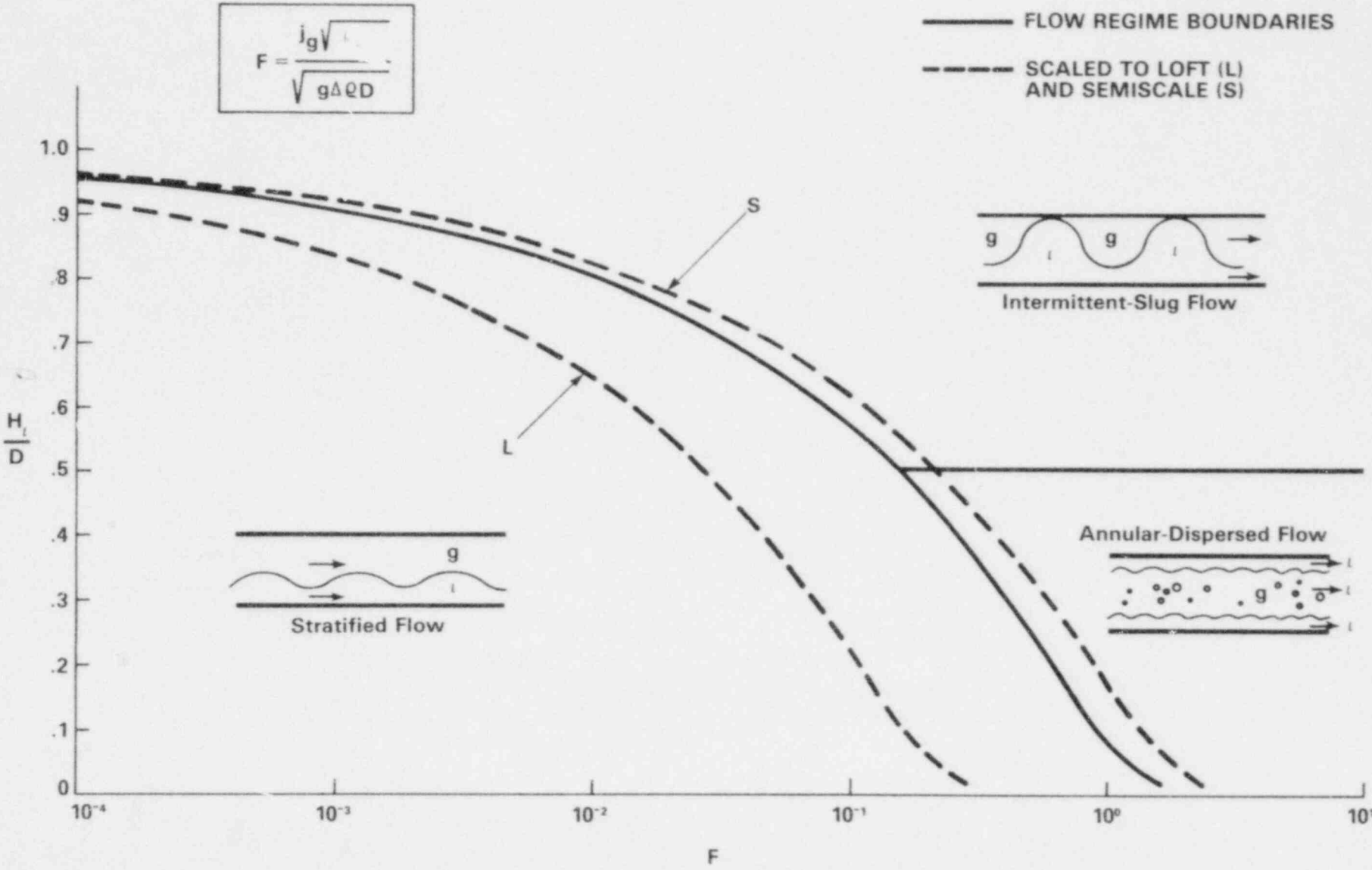

FIG. 2-1 DUKLER-TAITEL FLOW REGIME MAP

$$\alpha_m = \alpha_p \qquad 2\text{-}3$$

and of

$$\left(\frac{H_1}{D}\right)_m = \left(\frac{H_1}{D}\right)_p \qquad 2\text{-}4$$

between model and prototype.

Consequently, if geometric similarity is satisfied, it follows from Eq. 2-2 and Eq. 2-4, that flow regime transitions scale according to:

$$F_m = F_p \qquad 2\text{-}5$$

Thus, geometric similarity, that is, equality of void fractions implies Froude number equality and vice versa.

For a given fluid, if transitions occur at the same pressure, then Eq. 2-1 and Eq. 2-5 reduce to the following scaling rule:

$$\left(\frac{j_g}{\sqrt{D}}\right)_m = \left(\frac{j_g}{\sqrt{D}}\right)_p \qquad 2\text{-}6$$

2.2 Application to LOFT and Semiscale

The preceding results will be applied now to LOFT and Semiscale.

It is shown in Appendix B, that the power to volume scaling of LOFT and of Semiscale leads to the following relation between the vapor volumetric flux densities:

$$\frac{j_{gm}}{j_{gp}} = \frac{1}{S}\left(\frac{D_p}{D_m}\right)^2 \qquad 2\text{-}7$$

where S is the plant to model power ratio

$$S = \frac{\phi_p}{\phi_m} \qquad 2\text{-}8$$

Rewriting Eq. 2-1

$$F_m = \left(\frac{j_g \sqrt{\rho_g}}{\sqrt{g\Delta\rho D}}\right)_m \qquad 2\text{-}9$$

and substituting j_{gm} from Eq. 2-7 into Eq. 2-9, we get

$$\left(\frac{j_g \sqrt{\rho_g}}{\sqrt{g\Delta\rho D}}\right)_m = \frac{1}{S}\left(\frac{D_p}{D_m}\right)^{5/2}\left(\frac{j_g \sqrt{\rho_g}}{\sqrt{g\Delta\rho D}}\right)_p \qquad 2\text{-}10$$

It can be seen that Froude number scaling when combined with the power to volume scaling, results in a scale distortion given by

$$\Delta = \frac{1}{S}\left(\frac{D_p}{D_m}\right)^{5/2} \qquad 2\text{-}11$$

Table 2-1 below shows this distortion evaluated for hot legs of LOFT and Semiscale.

Table 2-1

	D(cm)	S	Δ
PWR	73.7	1	1
LOFT	28	64	0.176
Semiscale	3.4	1500	1.46

It can be seen that the value of Δ for a PWR is bounded by those corresponding to LOFT and to Semiscale.

The results are also plotted on Figure 2-1, where L stands for LOFT and S for Semiscale. We want to evaluate now the effect of scale distortion on the three facilities. We can distinguish two cases. One, in which all three systems: plant (P), LOFT (L) and Semiscale (S) have the same liquid depth (H_l/D). The other, in which all three have the same Froude number (F). Both are illustrated in Figure 2-2.

Consider the case of equal H_l/D which implies that the three systems have equal void fractions and are geometrically similar (see Appendix A). The constant liquid depth H_l/D, intersects the L, P, and S curves at three different values of F (see Figure 2-2). Thus, if conditions in the plant are such that a flow transition occurs say from separated to slug flow, then the hot leg of LOFT will have separated flow whereas Semiscale will have slug flow.

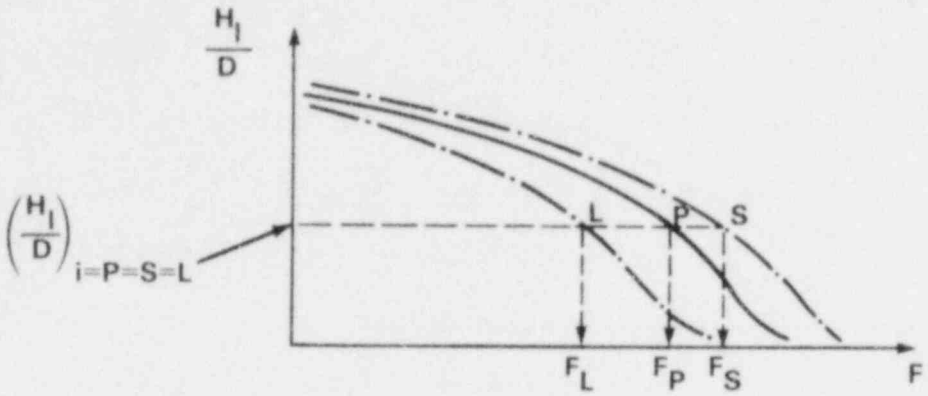

a. Preserving liquid depth, void fraction and time scale-effect on Froude number

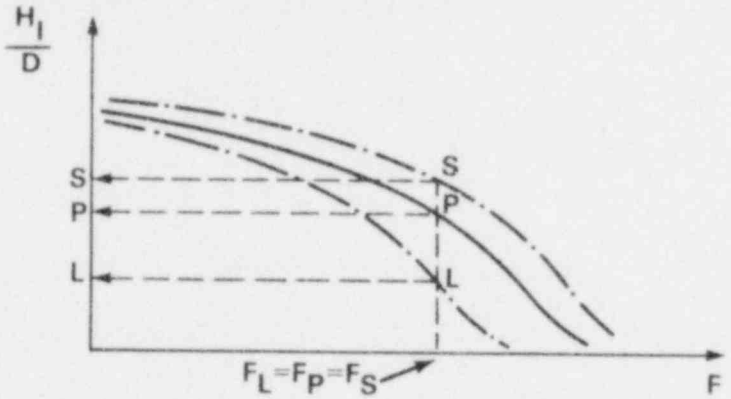

b. Preserving Froude number-effect on liquid depth

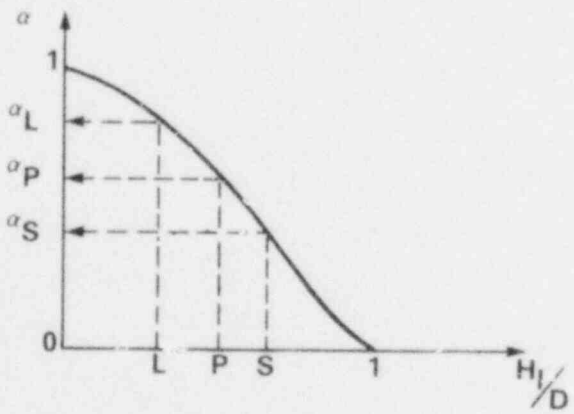

c. Preserving Froude number-effect on void fraction

FIG. 2-2 EFFECT OF DISTORTION

Consider now the case of equal Froude numbers. The line of constant F, intersects the P, L and S curves at three different values of H_l/D. This implies that the three systems will have different liquid depths and void fractions. Thus again, while a flow transition may take place in the hot leg of a plant, LOFT and Semiscale will have separated and slug flow respectively.

We conclude therefore, that Froude number scaling when used in conjunction with the power to volume scaling, leads to a distortion so that one cannot satisfy simultaneously geometric similarity (equality of void fractions) and equality of Froude numbers. If one is satisfied, the other is not and vice versa.

In order to make a quantitative estimate, let us assume that a hot leg in the plant is half full, that is, $(H_l/D)_p = 0.5$, therefore $\alpha_p = 0.5$. Figure 2-1 shows that this corresponds to a Froude number for the plant equal to $F_p = 0.157$. Values computed for LOFT and for Semiscale, corresponding to the two cases discussed above, are summarized in Table 2-2 and Table 2-3 below

Table 2-2

	H_l/D	α	F
PWR	0.5	0.5	0.157
LOFT	0.5	0.5	0.028
Semiscale	0.5	0.5	0.228

Table 2-3

	F	H_1/D	α
PWR	0.157	0.50	0.50
LOFT	0.157	0.12	0.95
Semiscale	0.157	0.56	0.49

The relation between H_1/D and α was determined from Figure A-2 in Appendix A.

It can be seen from these tables as well as from Figure 2-1, that flow regime transitions in a plant are bounded by those calculated for LOFT and Semiscale. Furthermore, these results indicate also that conditions leading to flow transitions in Semiscale are rather close to those which could be expected in a plant.

We want to determine now what is the effect of distortion on the time scale. It is known (see Ref. 1 through Ref. 3) that power to volume scaling preserves time. It is shown in Appendix C, that for separated two phase flow, time scales according to

$$\frac{t_m}{t_p} = \frac{\ell_m}{\ell_p} \sqrt{\frac{D_p}{D_m}} \sqrt{\left(\frac{H_1}{D}\right)_p \left(\frac{D}{H_1}\right)_m} \qquad 2\text{-}12$$

It was noted previously that when the Froude number scaling is used in conjunction with the power to volume scaling, one cannot satisfy simultaneously, geometric

similarity and equality of Froude numbers for model and prototype. This has also an effect on the time scale given by Eq. 2-12. Thus, if one satisfies the requirement of geometric similarity, then in view of Eq. 2-4, the scale of time becomes

$$\frac{t_m}{t_p} = \frac{\ell_m}{\ell_p} \sqrt{\frac{D_p}{D_m}} \qquad 2\text{-}13$$

Conversely, if one requires equality of Froude numbers then the ratio of liquid depths in Eq. 2-12, should be determined from Figure 2-1.

The results obtained by applying Eq. 2-13 to a PWR and Semiscale are shown in Table 2-4.

Table 2-4

	ℓ(cm)	D(cm)	t_m/t_p
PWR	770	73.7	1
Semiscale	247	3.4	1.49

The distortion is not very severe. Furthermore, as Eq. 2-13 indicates, the flow processes can be made isochronous by changing the dimensions of ducts so that

$$\frac{\ell_m}{\ell_p}\sqrt{\frac{D_p}{D_m}} = 1 \qquad 2\text{-}14$$

is satisfied.

It is important to note that the above analysis was based on the flow regime map proposed by Taitel and Dukler, Ref 5, which is valid for steady state only. In a second paper, Ref 6, these authors investigated experimentally and analytically the effect of flow transients. They show that "under transient conditions, flow pattern transient' can take place at flow rates substantially different then would occur under steady conditions." Since the equations described in Ref 6, require computer solution, in addition to specifying the pipe inlet conditions (which for Semiscale, LOFT and for a PWR, must be obtained from a system code), the effect of fast transients on flow regime transition and scaling was not considered in this report. However, for a small break LOCA this effect is not considered to be very significant because the process is quasi steady. Consequently, the results presented above may be used for the purpose of estimating the effect of flow regime transitions on the state of the fluid reaching the break.

2.3 Effect of Flashing

Since during a LOCA the pressure decreases, the question can be raised as to what is the effect of flashing on flow regimes? In other words, what is the effect of bubbles being present in the stratified liquid on the transition from stratified to slug flow or to annular - disperses flow? Such a process is illustrated in Figure 2-3.

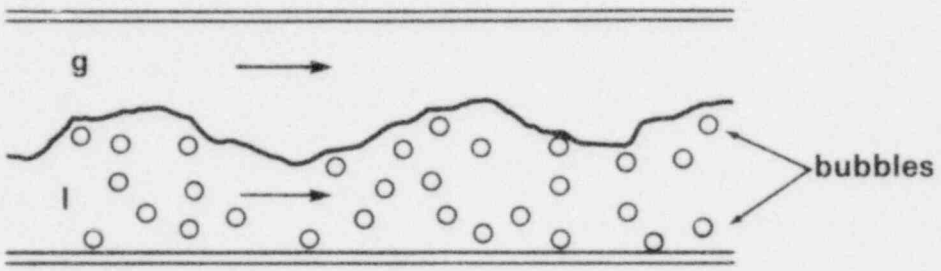

FIG. 2-3 EFFECT OF FLASHING ON SEPARATED FLOW

As discussed above, transitions from separated flow scale according to the vapor Froude number that is according to Eq. 2-2. If bubbles are present in the stratified liquid, this equation has to be modified to account for the decreased density of the lower fluid. Denoting by α_b, the void fraction due to bubbles in the liquid, then the density of the lower fluid instead of being equal to ρ_l, becomes

$$\rho_m = (1-\alpha_b)\,\rho_l + \alpha_b\,\rho_g \qquad 2\text{-}15$$

consequently instead of

$$\Delta\rho = \rho_l - \rho_g \qquad 2\text{-}16$$

which appears in Eq. 2-2, we should write

$$\rho_m - \rho_g = (1-\alpha_b)\,(\rho_l-\rho_g) = (1-\alpha_b)\,\Delta\rho \qquad 2\text{-}17$$

so that Eq. 2-2, becomes now

$$F = \frac{j_g\sqrt{\rho_g}}{\sqrt{g\Delta\rho(1-\alpha_b)D}} = f\left(\frac{H_l}{D}\right) \qquad 2\text{-}18$$

We conclude therefore that, for a given pressure and for a given liquid depth H_l/D, the effect of bubbles is to reduce the superficial vapor velocity j_g, required to induce a flow regime transition. This was to be expected in view of the Bernoulli effect.

2.4 Conclusion

1) With a break located above or below the interface in stratified two phase flow, a mixture rather than a single phase will be discharged through the break as consequence of flow regime transitions. According to available data in the literature, these transitions are scaled by Froude number for the vapor and by the void fraction. In particular, the results show that at a transition, the equality of Froude numbers between model and prototype implies geometric similarity, that is, equality of void fractions and vice versa.

2) It is shown that Froude number scaling when combined with the power to volume scaling of LOFT and of Semiscale, results in a scale distortion so that one cannot satisfy simultaneously geometric similarity and equality of Froude numbers. If one is satisfied the other is not and vice versa.

An evaluation of the effect of this distortion on modeling flow regimes in a hot leg of a PWR, LOFT and Semiscale indicates that flow regime transitions in a PWR are bounded by those of LOFT and of Semiscale. Furthermore, the results show that the calculated transitions for Semiscale are rather close to those which could be expected in a PWR on the basis of correlations available in the literature.

3) It is shown that because of this distortion the scale of time is not preserved, that is, flow processes in model and prototype are not isochronous. For Semiscale this effect is not very severe. It is shown

also that by changing duct geometry, these processes can be made to be isochronous.

4) It is shown that the effect of bubbles in the stratified liquid is to reduce the vapor flux required to induce a flow regime transition. This decrease is to be expected in view of the Bernoulli effect. The flow regime transition criterion proposed by Dukler and Taitel, was modified to account for the presence of bubbles.

3. Liquid Entrainment in the Break

3.1 Scaling

When the break is located above the horizontal interface, liquid can be entrained in break flow as a consequence of flow regime transitions analyzed in the preceding section, or due to vapor acceleration (Bernoulli effect) in the vicinity of the break. The latter is illustrated in Fig. 3-1. No information, either from experiments or analysis, was found in the literature dealing with the processes illustrated in Fig. 3-1.

However, experimental data and analyses are available in the literature which deal with liquid withdrawal from a large reservoir through a side orifice or slot, and through a vertical pipe. Both are shown in Fig 3-2, together with criteria for incipient liquid entrainment through side orifices

$$\frac{V_g \sqrt{\rho_g}}{\sqrt{g\Delta\rho L_g}} \geq 3.25 \left(\frac{L_g}{d}\right)^2 \qquad 3\text{-}1$$

and through slots

$$\frac{V_g \sqrt{\rho_g}}{\sqrt{g\Delta\rho L_g}} \geq 1.52 \left(\frac{L_g}{d}\right) \qquad 3\text{-}2$$

derived analytically by Craya, Ref 7, and verified experimentally by Gariel, Ref 8. This figure shows also the criterion for entrainment in the vertical direction, proposed by Rouse, Ref 9,

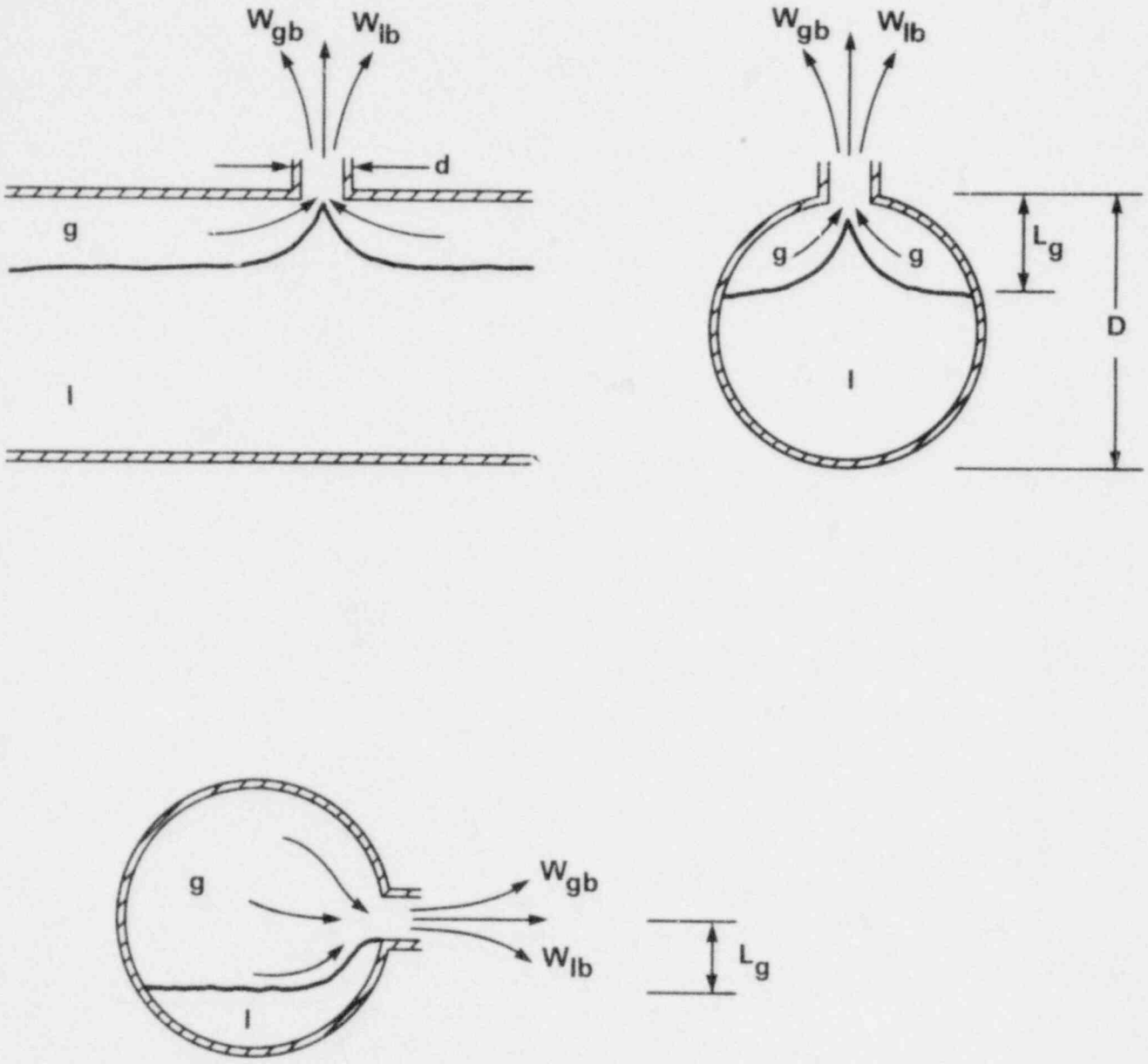

FIG. 3-1 ILLUSTRATION OF LIQUID ENTRAINMENT IN BREAK FLOW DUE TO BERNOULLI EFFECT

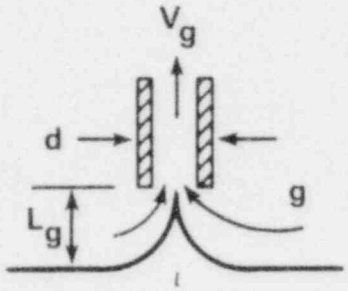

$$\frac{V_g\sqrt{\varrho_g}}{\sqrt{g\Delta\varrho L_g}} \geq 5.7\left(\frac{L_g}{d}\right)^{3/2}$$

a. Liquid withdrawal through vertical pipe.
Correlation for incipient withdrawal - Ref. 9

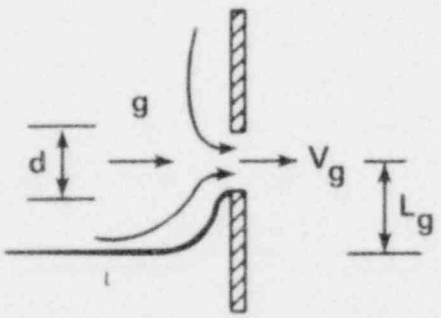

Orifice: $$\frac{V_g\sqrt{\varrho_g}}{\sqrt{g\Delta\varrho L_g}} \geq 3.25\left(\frac{L_g}{d}\right)^2$$

Slot: $$\frac{V_g\sqrt{\varrho_g}}{\sqrt{g\Delta\varrho L_g}} \geq 1.52\left(\frac{L_g}{d}\right)$$

b. Liquid withdrawal through side orifice and/or slot.
Correlations for incipient withdrawal - Ref. 7 and Ref. 8

FIG. 3-2 LIQUID WITHDRAWAL DUE TO BERNOULLI EFFECT

$$\frac{V_g \sqrt{\rho_g}}{\sqrt{g\Delta\rho L_g}} \geq 5.7 \left(\frac{L_g}{d}\right)^{3/2} \qquad 3\text{-}3$$

It is realized that the results in these references do not correspond to PWR conditions. For example, the experiments were conducted with two incompressible fluids at atmospheric pressure, neither the effects of pipe geometry nor of the liquid flow were accounted for etc. Nevertheless, these results are useful for several reasons.

First, Eq 3-1, Eq 3-2, and Eq 3-3, show that break location with respect to the interface (side or vertical withdrawal) and break geometry (orifice or slot) have an important effect on scaling the conditions for incipient liquid entrainment. Note, that these two parameters determine the relation between the vapor Froude number (based on vapor velocity through the outlet) and the L_g/d ratio. Consequently, one should not expect that a single criterion will describe incipient liquid entrainment through breaks in horizontal pipes.

Secondly, for small breaks in large pipes, the effect of pipe curvature on the velocity field in the vicinity of the break in not very large. Consequently, the flow through an orifce located in a vertical plane (such as illustrated in Fig. 3-2) may be a satisfactory approximation to the flow through a break on the side (at 90°) of a pipe. A similar argument can be made for a break located at the top (at 0°) of the pipe. Furthermore, in small breaks, the velocity of the liquid is small when compared to the vapor velocity in the vicinity of the break, so that in relation to this vapor, one could assume that the liquid is stagnant.

These observations lead us to conclude that although Eq 3-1, Eq 3-2 and Eq 3-3, do not correspond exactly to PWR conditions, they still may be useful for the purpose of estimating incipient liquid entrainment through breaks in a PWR, LOFT and Semiscale. This will be done in the section that follows.

3.2 Application to LOFT and Semiscales

Incipient liquid entrainment criteria listed in the preceding section are all of the form

$$\frac{V_g \sqrt{\rho_g}}{\sqrt{g\Delta\rho L_g}} \geq C \left(\frac{L_g}{d}\right)^m \qquad 3\text{-}4$$

where the constant C and exponent m = 1, 3/2, 2 depend on the location and geometry of the outlet.

Assuming that the process in the plant and in the model occurs at the same pressure and that the vapor flow through the break is choked, then

$$V_{gm} = V_{gp} \qquad 3\text{-}5$$

and Eq 3-4 leads to the following scaling relation

$$\frac{L_{gm}}{L_{gp}} = \left(\frac{d_m}{d_p}\right)^{m/m + 1/2} \qquad 3\text{-}6$$

which can be expressed also as

$$\left(\frac{L_g}{D}\right)_m = \left(\frac{d_m}{d_p}\right)^{m/m + 1/2} \frac{D_p}{D_m} \left(\frac{L_g}{D}\right)_p \qquad 3\text{-}7$$

It is shown in Appendix A, that in separated flow, the requirement of geometric similarity, that is, of equal void fractions, implies, also the equality

$$\left(\frac{L_g}{D}\right)_m = \left(\frac{L_g}{D}\right)_p \qquad 3\text{-}8$$

It follows therefore from Eq 3-7, that the scale distortion is given by

$$\Delta = \left(\frac{d_m}{d_p}\right)^{m/m + 1/2} \frac{D_p}{D_m} \qquad 3\text{-}9$$

Table 3-1, below shows the results of applying Eq 3-6 and Eq 3-9, to a PWR, LOFT and Semiscale for the case of a side orifice, that is for m = 2.

Table 3-1

	D (cm)	d (cm)	L_{gm}/L_{gp}	Δ
PWR	73.7	11.4	1	1
LOFT	28	1.62	0.21	0.55
Semiscale	3.4	0.28	0.052	1.12

This table indicates that the calculated incipient liquid entrainment in a PWR, is bounded by those calculated for LOFT and Semiscale.

In order to estimate the range of L_g/d, over which one could expect liquid entrainment in the hot leg of a PWR, we use the criterion for incipient liquid entrainment through a side orifice, that is, Eq 3-1, which can be expressed also as

$$\frac{V_g \sqrt{\rho_g}}{\sqrt{g\Delta\rho d}} \geq 3.25 \left(\frac{L_g}{d}\right)^{2.5} \qquad 3\text{-}10$$

At 1000 psia, the critical velocity for the vapor is aproximately 500 m/sec, and with a break diameter equal to d = 11.4 cm, Eq 3-10, yields

$$\frac{L_g}{d} < 4.5 \qquad 3\text{-}11$$

Consequently, liquid entrainment would cease when the liquid level has reached a distance of approximately 51 cm below the break center. This is rather high, more than one would have expected. Perhaps, the value of the constant and/or of the exponent in Eq. 3-10, are not strictly applicable to pipe flow. It is evident that experimental data would be needed to resolve this question. Nevertheless, the results indicate a high propensity for liquid entrainment.

3.3 Conclusions

(1) With a break located above the interface, liquid can be entrained in break flow as a consequence of vapor acceleration in the vicinity of the break. No data were found in the literature dealing with this process.

(2) However, experimental data and analyses were found which deal with liquid withdrawal from large reservoirs through a side orifice or slot, and through a vertical pipe. They show that break location with respect to the interface as well as break geometry have an important effect on correlations which predict incipient liquid entrainment through a break.

(3) An application of available correlations to PWR, LOFT and Semiscale indicates a high propensity for liquid entrainment. Furthermore, the results show that conditions for incipient liquid entrainment calculated for a PWR are bounded by those scaled to LOFT and Semiscale.

4. Vapor Pull-Through

With a break located below the horizontal interface, vapor can reach the break because of vortex formation or by being pulled-through in a vortex free flow. Both processes are illustrated in Fig. 4-1. No information was found in the literature on these processes for conditions of interest to a PWR. Specifically, data on incipient vapor pull-through for pipe flow at high pressures were not found.

However, experimental data and correlations are available on incipient pull-through drains in large reservoirs for vortex as well as for vortext free flows. These correlations are useful because they indicate the form of scaling relations. Furthermore, when liquid velocities are low, as in the case for small break LOCA's, one could use the available correlations (valid for draining large reservoirs) and apply them to facilities of interest in order to estimate the conditions which may lead to incipient vapor pull-through. This will be done in the two sections that follow.

4.1 Vortex Flow

Experimental data and analyses are available which deal with vortex motion in draining liquids. In what follows we shall use the results reported by Daggett and Keulegan, Ref. 10, and by Plesset, Ref. 11.

The authors of Ref. 10, present data and correlations for predicting incipient vapor pull-through due to a vortex reaching the drain at the bottom of a

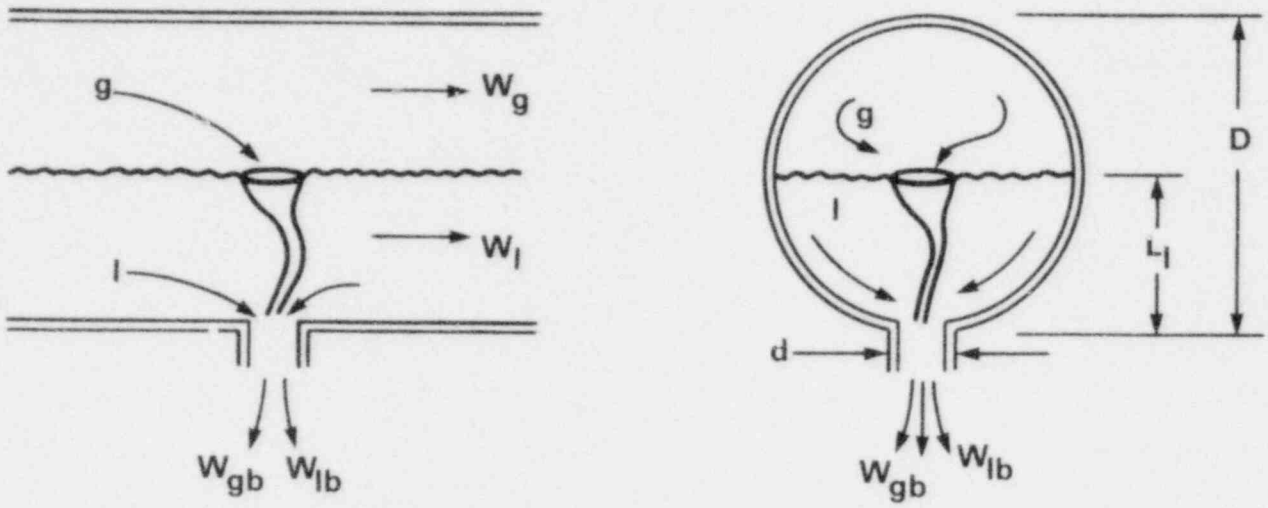

a. Vapor pull-through due to vortex formation

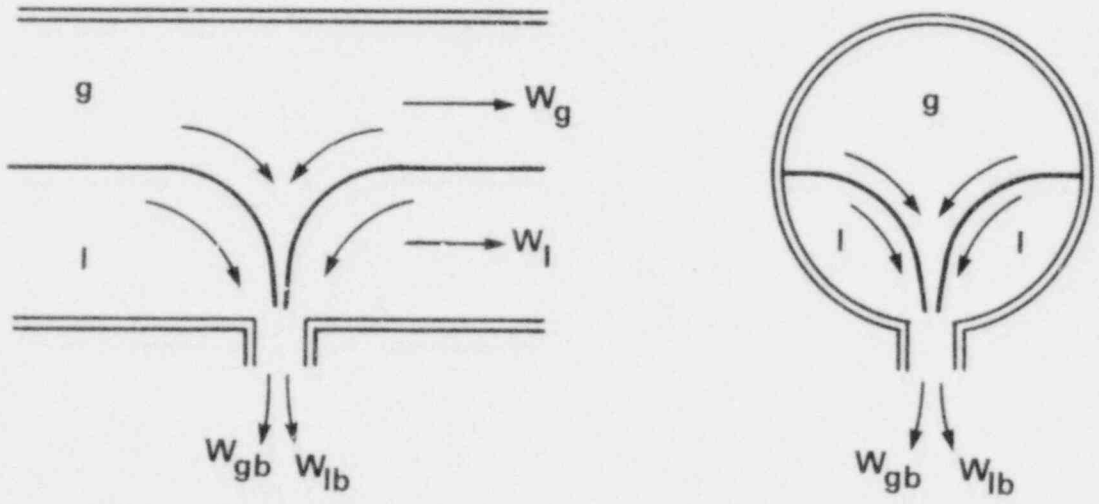

b. Vapor pull-through in vortex-free flow

FIG. 4-1 ILLUSTRATIONS OF MECHANISMS FOR VAPOR PULL-THROUGH A BREAK

vessel. Using the nomenclature shown in Fig. 4-1, where Γ, stands for the initial circulation and V for the velocity of the liquid at the drain, Daggett and Keulegan proposed the following correlations

$$\frac{L_\ell}{d} \leq 17.5 \times 10^{-3} \frac{\Gamma}{\nu_\ell} \qquad 4\text{-}1$$

for

$$\frac{Vd}{\nu_\ell} < 3.3 \times 10^4$$

and

$$\frac{\Gamma}{VL_\ell} \geq \frac{\Pi}{150} \qquad 4\text{-}2$$

for

$$\frac{Vd}{\nu_\ell} > 3.3 \times 10^4$$

In order to use these correlations we have to estimate first the Reynolds number. Assuming choked flow at the break, at 1000 psia the velocity is approximately 20 m/sec. and with d = 0.23 cm we obtain for Semicale

$$\frac{Vd}{\nu_\ell} = 4.25 \times 10^5 \qquad 4\text{-}3$$

Consequently, we should use Eq. 4-2, which indicates that incipient vapor pull-through is <u>independent</u> of the break size.

Assuming that the processes in the model and in the plant take place at the same pressure, Eq. 4-2 reduces to the scaling relation given below

$$\frac{L_{\ell m}}{L_{\ell p}} \leq \frac{\Gamma_m}{\Gamma_p} \qquad 4\text{-}4$$

In order to proceed one needs data and/or relations for calculating the circulation Γ. Such information is not available for conditions of intersst. In what follows we shall use the scale of circulation proposed by Plesset, Ref. 11, given by

$$\Gamma \sim d\sqrt{gL_\ell} \qquad 4\text{-}5$$

Substituting Eq. 4-5 in Eq. 4-4 yields the ratio (model to prototype) of liquid depths for conditions of incipient pull-through due to vortext flow at the break, thus

$$\frac{L_{\ell m}}{L_{\ell p}} \leq \left(\frac{d_m}{d_p}\right)^2 = \frac{1}{S} \qquad 4\text{-}6$$

which can be expressed also as

$$\left(\frac{L_\ell}{D}\right)_m = \frac{1}{S} \quad \frac{D_p}{D_m} \quad \left(\frac{L_\ell}{D}\right)_p \qquad 4\text{-}7$$

Since for geometric similarity, that is, for equal void fraction we have (see Appendix A)

$$\left(\frac{L_\ell}{D}\right)_m = \left(\frac{L_\ell}{D}\right)_p \qquad 4\text{-}8$$

we obtain from Eq. 4-7, the distortion

$$\Delta = \frac{1}{S} \quad \frac{D_p}{D_m} = \left(\frac{d_m}{d_p}\right)^2 \left(\frac{D_p}{D_m}\right) \qquad 4\text{-}9$$

Table 4-1, below shows the distortion evaluated for a hot leg of a PWR, LOFT and Semiscale

Table 4-1

	D cm	S	Δ
PWR	73.7	1	1
LOFT	28	64	0.041
Semiscale	3.4	1500	0.015

From these results and Eq. 4-7, it appears that incipient vapor pull-through due to vortex formation, will occur at a greater liquid depth, (L_ℓ/D), that is, at lower void fractions α, in a PWR than in either LOFT or Semiscale. In other words, these results indicate that a PWR has a higher propensity for vapor pull-through than either LOFT or Semiscale.

4.2 Vortex Free Flow

Several references are available which present experimental data and analyses of vapor pull through in vortex free flow during drainage of tanks. In what follows we shall use the results reported by Lubin and Hurwitz, Ref. 12.

These authors present experimental data together with an analysis of the vortex free pull through mechanism. Two correlations for predicting incipient pull-through conditions, were derived and verified experimentally. These were

$$\frac{V\sqrt{\rho_\ell}}{\sqrt{g\Delta\rho d}} \geq 2.3 \left(\frac{L_\ell}{d}\right)^{3/2} \qquad 4\text{-}10$$

for

$$\frac{L_\ell}{d} < 1$$

and

$$\frac{V\sqrt{\rho_\ell}}{\sqrt{g\Delta\rho d}} \geq 3.25 \left(\frac{L_\ell}{d}\right)^{5/2} \qquad 4\text{-}11$$

for

$$\frac{L_\ell}{d} > 1$$

Both correlations are plotted on Fig. 4-2, with $L_\ell = H_\ell$, since the break is at the bottom.

Assuming that the processes in model and prototype occur at the same pressure and that the flow at the break is choked, Eq. 4-10 leads to the following scaling relation when $L_\ell/d < 1$

$$\frac{L_{\ell m}}{L_{\ell p}} = \left(\frac{d_m}{d_p}\right)^{2/3} = \frac{1}{S^{1/3}} \qquad 4\text{-}12$$

or

$$\left(\frac{L_\ell}{D}\right)_m = \frac{1}{S^{1/3}} \frac{D_p}{D_m} \left(\frac{L_\ell}{D}\right)_p \qquad 4\text{-}13$$

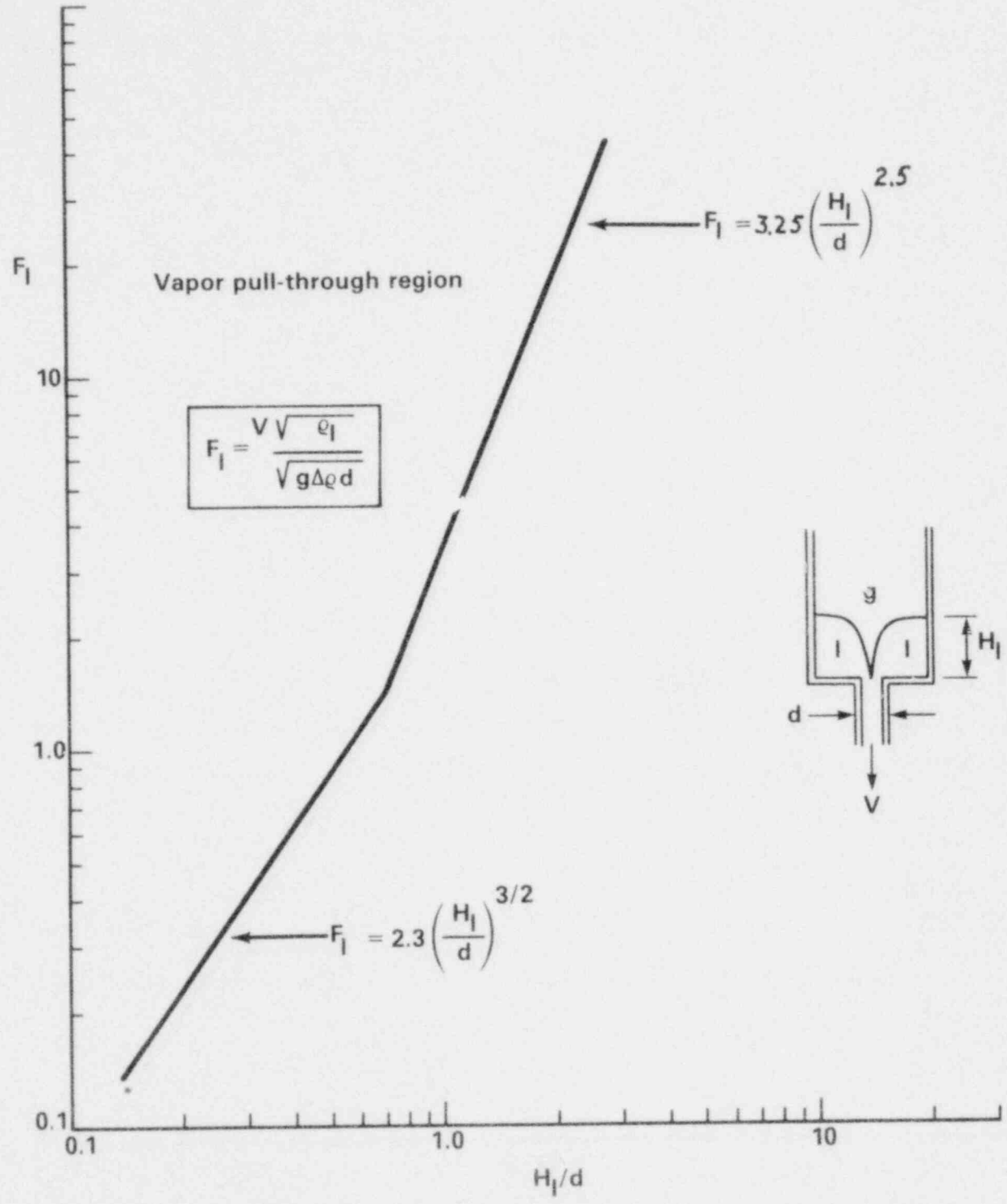

FIG. 4-2 CORRELATION FOR INCIPIENT VAPOR PULL-THROUGH IN VORTEX-FREE FLOW - REF. 12

from which we obtain the scale distortion:

$$\Delta_1 = \frac{1}{S^{1/3}} \quad \frac{D_p}{D_m} \qquad 4\text{-}14$$

whereas, when $L_{\ell/d} > 1$, we have from Eq. 4-11

$$\frac{L_{\ell m}}{L_{\ell p}} = \left(\frac{d_m}{d_p}\right)^{4/5} = \frac{1}{S^{2/5}} \qquad 4\text{-}15$$

or

$$\left(\frac{L_\ell}{D}\right)_m = \frac{1}{S^{2/5}} \quad \frac{D_p}{D_m} \left(\frac{L_\ell}{D}\right)_p \qquad 4\text{-}16$$

whence the scale distortion

$$\Delta_2 = \frac{1}{S^{2/5}} \left(\frac{D_p}{D_m}\right) \qquad 4\text{-}17$$

Table 4-2 below, shows the two distortions evaluated for the hot leg of a PWR, LOFT and Semiscale

Table 4-2

	D (cm)	S	Δ_1	Δ_2
PWR	73.7	1	1	1
LOFT	28	64	0.656	0.53
Semiscale	3.4	1500	1.89	1.16

The results indicate that conditions which may lead to a vapor pull-through in a PWR are bounded by those scaled to LOFT and Semiscale.

If we assume that the prototype and model have the same void fraction and that the conditions in the plant correspond to incipient pull-through, then these result indicated that vapor will be pulled through in LOFT but not in Semiscale.

We shall estimate now the conditions for vapor pull-through in a PWR. Assuming again that the velocity of the choked flow is approximately equal to 20 m/sec, we find for a break diameter equal to d = 11.4 cm, that

$$\frac{V\sqrt{\rho_\ell}}{\sqrt{g\Delta\rho d}} \approx 20 \qquad 4\text{-}18$$

and Fig. 4-2, shows that vapor pull-through will occur if

$$\frac{L_\ell}{d} < 2.1 \qquad 4\text{-}19$$

that is, when the depth of the liquid above the break is less than approximately 24 cm. Although this value may not be exact, nevertheless the results indicate a propensity for pull-through.

4.3 Conclusions

1. With a break located below the horizontal liquid interface, vapor can reach the break due to vortex formation or by being pulled through in a

vortex free flow. No data were found in the literature on these processes for conditions of interest to PWR.

2. However, experimental data and correlations are available in the literature on incipient pull-through for both vortex and vortex free flows during drainage of tanks.

3. An application of correlations for vortex flow, indicates that for conditions of interest to a PWR, LOFT and Semiscale, incipient pull-through does not depend on break size. The results also indicate that both LOFT and Semiscale have a lower propensity for vapor pull through due to vortex flow, than a PWR.

4. An application of correlations proposed for vortex free flow, indicates that incipient pull through conditions in a PWR are bracketted by those scaled to LOFT and Semiscale. Furthermore, these results also indicate a considerable propensity for vapor pull through a small break in a PWR. For example, for a break diameter equal to 11.4 cm vapor pull-through will occur when the depth of the liquid above the break is approximately 24 cm or less.

5. Counter Current Flow Limitation in Horizontal Pipes

5.1 Scaling

In a small break LOCA, the steam generator may operate in a "reflux boiler" mode, so that liquid condensing in the primary side will flow through the ho leg back into the core. This return flow is gravity dominated. Since the liquid and the vapor are in counter current flow, the question arises as to whether or not the CCFL phenomenon can occur. This question is important because if CCFL can occur, then the liquid may be prevented from flowing back into the core. It is evident that CCFL can have an effect on the distribution of the liquid in the system and, therefore, on the inventory in the core.

Experimental data on CCFL phenomena in horizontal pipes, applicable to PWR conditions were not found in the literature.

However, Wallis Ref. 1, reported data on flooding for air-water flowing through a horizontal, rectangular (2.54 cm x 2.54 cm) channel. The experimental results were correlated by equation:

$$\frac{j_g\sqrt{\rho_g}}{\sqrt{g\Delta\rho D}} = \frac{1}{2}\,\alpha^{3/2} \qquad 5\text{-}1$$

Visual observation of the CCFL process indicated that it is associated with an instability of long waves. Indeed, as Wallis noted Eq. 5-1 is in agreement

with theoretical results reported by many authors who analyzed the stability of stratified (two-fluid) flows.

Additional experimental data and analyses of stratified flows, which may be of interest to the present problem, are available in the literature. They are concerned with gravity or density currents, that is, with the intrusion of a heavy fluid into a mass of a lighter fluid illustrated in Figure 5-1. This phenomenon occurs in meteorology when a cold front moves in; and in hydrology, when a muddy water or salt-water intrude into a mass of fresh water.

Von Karman, Ref. 14, derived an equation for the speed V of propagation of a density front

$$\frac{V\sqrt{\rho_2}}{\sqrt{g\Delta\rho H_1}} = 1 \qquad 5\text{-}2$$

the notation is shown in Figure 5-1. Whereas, Keulegan, Ref. 15, and Grubert, Ref. 16, presented experimental data and correlations for calculating the length, L_o, of an arrested wedge:

$$\frac{L_o}{H} = \frac{1}{30}\left(\frac{H}{\nu_2}\sqrt{\frac{g\Delta\rho H}{\rho_1}}\right)^{0.5}\left(\frac{V_1\sqrt{\rho_1}}{\sqrt{g\Delta\rho H}}\right)^{-2.5} \qquad 5\text{-}3$$

Where ν_2 is the kinematic viscosity of phase 2.

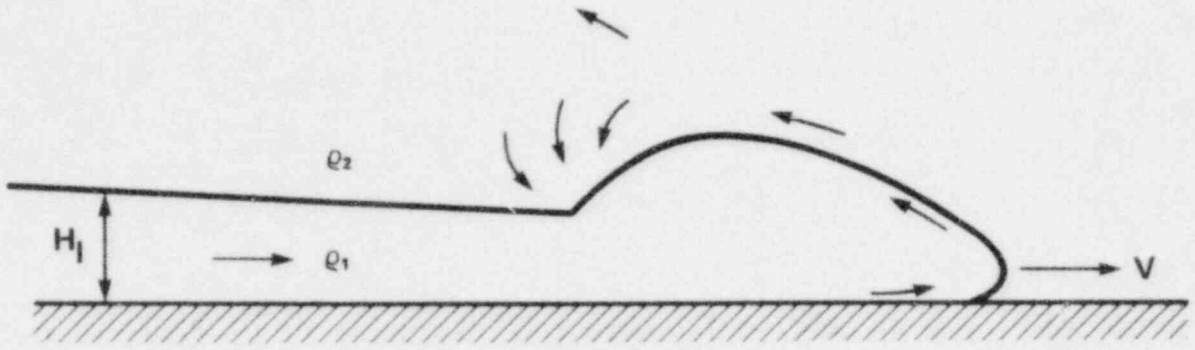

a. Advancing Front

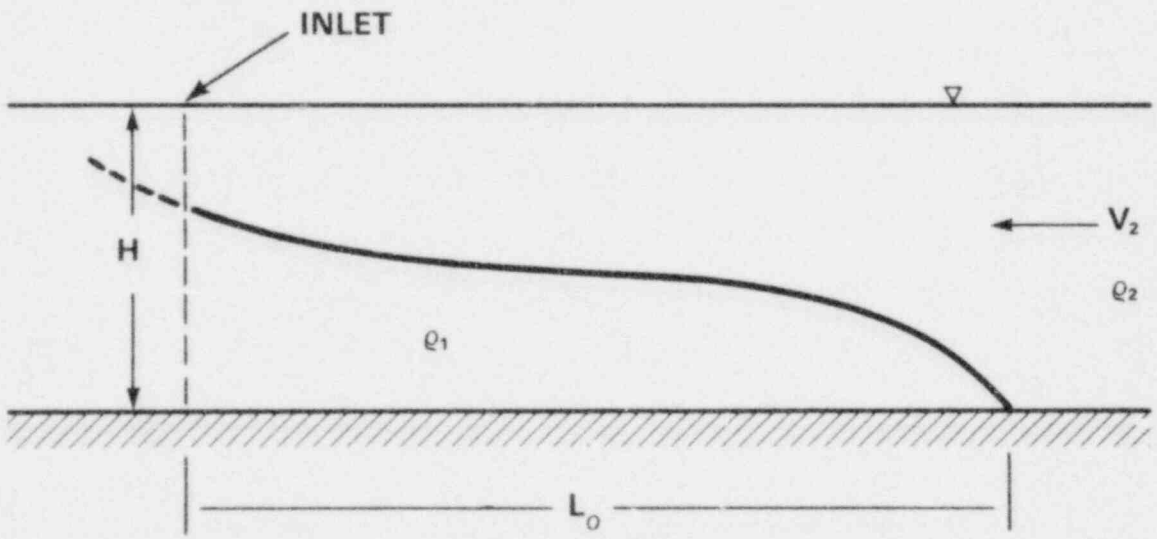

b. Arrested Wedge

FIG. 5-1 DEFINITION OF NOTATIONS

The notation is illustrated again in Figure 5-1.

It is realized that the results reported in Ref. 13 through Ref. 16, do not correspond to PWR conditions. Nevertheless, the results reported in these references are useful because they indicate the form of correlations for calculating processes that bear a similarity to those under consideration here. Consequently, the equations above will be used in the section that follows to estimate the conditions which may lead to CCFL, in a hot leg of a PWR, LOFT and Semiscale.

5.2 Applications to LOFT and Semiscale

It can be seen that Eq. 5-1, is of the same form as Eq. 2-1, that is, the CCFL correlation in horizontal pipes obeys the Froude number scaling. Consequently, when used in conjunction with the power to volume scaling of LOFT and Semiscale, it will lead to a distortion given by Eq. 2-11, which is evaluated in Table 2-1. Figure 5-2 shows Eq. 5-1 together with the results scaled to LOFT and Semiscale. It indicates that conditions which may lead to CCFL in a PWR, are bounded by those calculated for LOFT and Semiscale. As in the case of Eq. 2-10, these results show also that because of this distortion, one cannot satisfy simultaneously the equality of Froude numbers and of geometric similarity, that is, equality of void fractions for the three facilities. This conclusion could be illustrated in Figure 5-2, in the same way as it was done in Figure 2-2.

In order to obtain a quantitative estimate of conditions that may lead to CCFL in a PWR, we shall assume a void fraction of $\alpha_p = 0.5$. Taking the pressure of

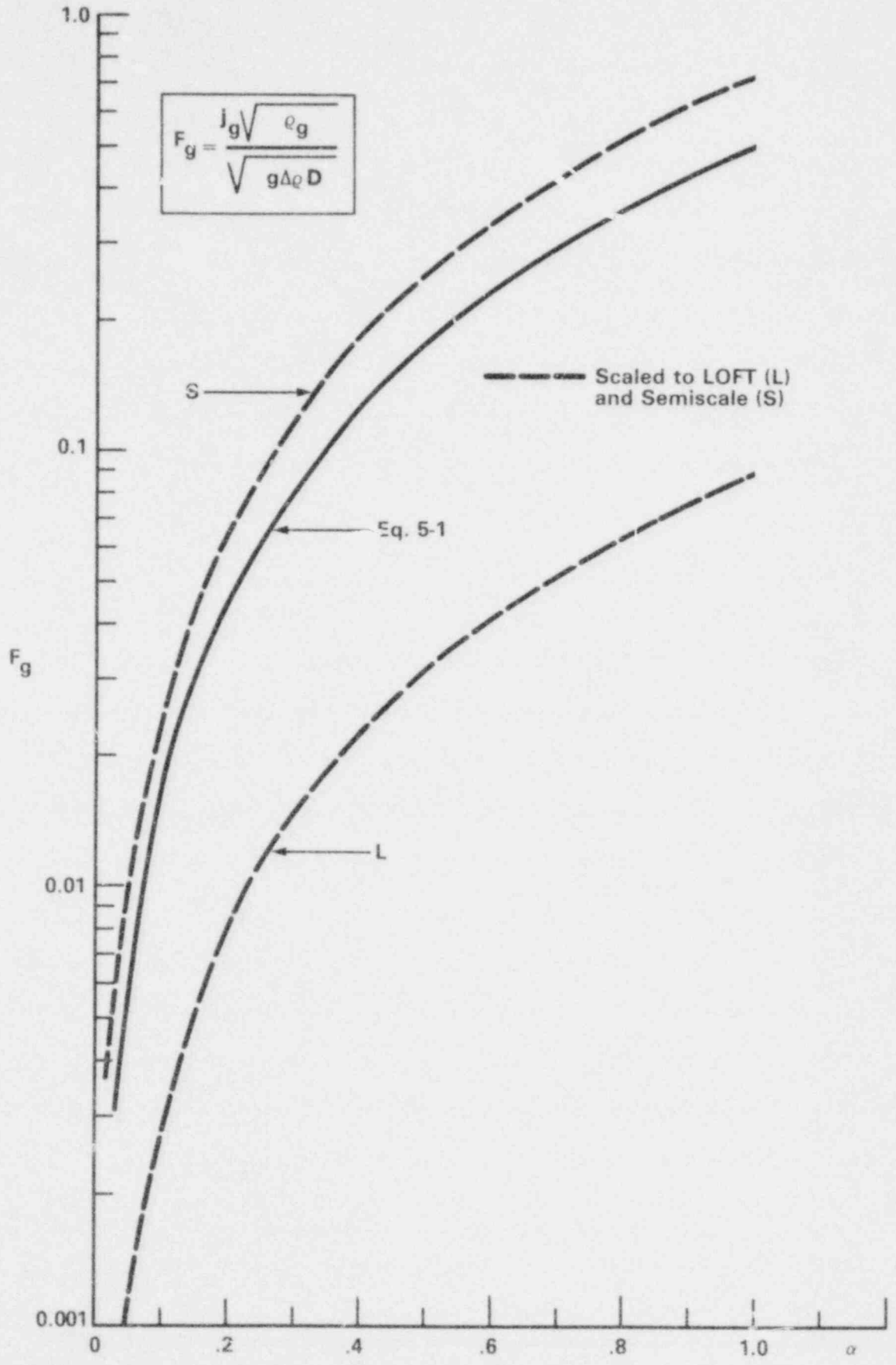

FIG. 5-2 FLOODING CORRELATION
IN HORIZONTAL PIPES - REF. 13

1000 psia and with D = 73.7 cm, we obtain from Eq. 5-1, the mass flux of vapor G_g = 15.7 lb/sec ft^2 which is equivalent to a power of 1.04 x 10^4 Btu/sec. These are surprisingly low values. Although, they may not be exact, nevertheless, they tend to indicate a high propensity for CCFL phenomena occurring in a hot leg of a PWR.

Before applying Eq. 5-2 and Eq. 5-3, perhaps we ought to describe briefly the similarity between the phenomena they model and the present problem. As vapor condenses in the steam generator, it will flow through the hot leg back into the core. This flow is gravity dominated. Under some conditions (if the hot leg was initially dry) we can visualize this flow as a liquid front (wedge) advancing through the hot leg. As noted above, Eq. 5-2 predicts the speed at which a denser fluid will propagate through a lighter one. While Eq. 5-3 predicts the distance (from the inlet) for the dense fluid wedge to be arrested by a lighter fluid flowing in the opposite direction.

For an advancing wedge to be arrested, it is necessary to super-impose a flow of the lighter fluid in the opposite direction. According to Eq. 5-2, this flow scales as:

$$\frac{j_g\sqrt{\rho_g}}{\sqrt{g\Delta\rho D}} = \sqrt{\frac{H_\ell}{D}} \qquad 5\text{-}4$$

it obeys therefore, Froude number scaling. It can be seen that this equation is of the same form as Eq. 2-2. Consequently, the comments and conclusions

made with respect to the latter, apply also to Eq. 5-4. For example, the distortion is given by Eq. 2-11, which would indicate that the condition for arresting an advancing liquid wedge in a hot leg of a PWR is bounded by those scaled to LOFT and Semiscale. Specifically, if in a PWR the wedge is at the point of being arrested, in LOFT it would still advance, while in Semiscale it would have been already arrested.

In order to estimate the length of a liquid wedge arrested by the vapor flowing in the opposite direction, we use Eq. 5-3 expressed in the nomenclature of this report:

$$\frac{\ell_o}{D} = \frac{1}{30}\left(\frac{D}{\bar{v}_g}\sqrt{\frac{g\Delta\rho D}{\rho_\ell}}\right)^{0.5}\left(\frac{1}{j_g}\sqrt{\frac{g\Delta\rho D}{\rho_\ell}}\right)^{2.5} \qquad 5\text{-}5$$

If the pressure is the same in model and prototype we obtain then the following scaling relation:

$$\left(\frac{\ell}{D}\right)_m = \left(\frac{j_p}{j_m}\right)^{2.5}\left(\frac{D_m}{D_p}\right)^{2}\left(\frac{\ell}{D}\right)_p \qquad 5\text{-}6$$

which in view of Eq. 2-7, can be expressed also as

$$\left(\frac{\ell}{D}\right)_m = S^{2.5}\left(\frac{D_m}{D_p}\right)^{7}\left(\frac{\ell}{D}\right)_p \qquad 5\text{-}7$$

the distortion is then

$$\Delta = S^{2.5} \left(\frac{D_m}{D_p} \right)^7 \qquad 5\text{-}8$$

Table 5-1 below shows this distortion evaluated for the hot legs of LOFT and Semiscale.

Table 5-1

	D(cm)	S	Δ
PWR	73.7	1	1
LOFT	28	64	36
Semiscale	3.4	1500	0.39

The results indicate again, that the calculations for a PWR are bounded by those pertaining to LOFT and to Semiscale.

To make an order of magnitude estimate of this arresting length, let us assume a decay power of 7.55×10^3 Btu/sec, which at 1000 psia corresponds to a vapor mass flow of $W_g = 116.5$ lb/sec and with a pipe diameter of D = 73.7 gives a vapor Reynolds number equal to 4.65×10^6. The superficial vapor velocity being approximately $j_g = 350$ cm/sec, Eq. 5-3 yields for the ratio

$$\frac{\ell}{D} \simeq 32$$

whence the length is $\ell \simeq 82$ ft. Since in a plant the length is of the order of 25 ft, we could conclude that for the assumed conditions, the liquid could flow back into the core.

5.3 Conclusions

1) Experimental data on CCFL phenomena in horizontal pipes, applicable to PWR conditions were not found in the literature.

2) However, some data are available on air-water flooding in a rectangular (1 in x 1 in) duct, as well as on the propagation of density fronts and on their length when arrested.

3) Available data on air-water flooding in horizontal ducts indicate that the process induced by an instability of long waves, is scaled by the vapor Froude number. The latter being a function of void fraction.

   An application of the proposed correlation indicates that conditions which may lead to CCFL in a PWR are bounded by those scaled to LOFT and Semiscale. These results also indicate a potential for CCFL phenomena occurring in a PWR.

4) Available correlations for calculating the length of an arrested liquid wedge show that this length is a strong function of the velocity of the lighter phase. The correlation indicates that the condition for arresting an advancing liquid wedge in a hot leg of a PWR is bounded by those

scaled to LOFT and Semiscale. Specifically, if in a PWR the wedge is at the point of being arrested, in LOFT it would still advance, while in Semiscale it would have been already arrested.

6. Conclusions

Each preceding section presents a list of conclusions pertaining to a particular process. Here we shall summarize only those which are concerned with facilities.

6.1 Flow Regime Transitions

1) It was shown that Froude number scaling when combined with the power to volume scaling of LOFT and of Semiscale results in a scale distortion (see Eq. 2-11). Calculations indicate that conditions which may lead to flow regime transitions in a PWR are bounded by those scaled to LOFT and Semiscale (see Figure 2-1 and Tables 2-1 through Table 2-3).

2) It was shown that because of this distortion the scale of time is not preserved, that is, flow processes in model and prototype are not isochronous. For Semiscale this effect is not severe (see Table 2-4).

3) It was shown that the effect of flashing is to reduce the vapor flux required to induce a flow regime transition. The flow regime transition criterion proposed by Dukler and Taitel was modified to account for this effect (see Eq. 2-18).

6.2 Liquid Entrainment at the Break

1) For PWR conditions, no data were found in the literature dealing with the processes illustrated in Figure 3-1. However, experimental data and

correlations on liquid withdrawal from large reservoirs (see Figure 3-2) indicate that break location with respect to the interface, as well as break geometry have an important effect on incipient liquid entrainment.

2) An application of these correlations (see Equation 3-2) to PWR, LOFT and Semiscale indicates a high propensity for liquid entrainment (see Eq. 3-11). The results show also (see Table 3-1) that conditions which may lead to incipient liquid entrainment in a PWR, are bracketted by those scaled to LOFT and Semiscale.

6.3 Vapor Pull-Through

1) For conditions of interest to a PWR, no experimental data were found in the literature dealing with incipient vapor pull-though due to vortex formation. Data are available, however, on vortex effects during the drainage of large vessels (see Equation 4-1 and Equation 4-2).

An application of these correlations indicates that for conditions of interest to a PWR, LOFT and Simiscale, incipient pull-through does not depend on break size (see Equation 4-2). The results also indicate (see Table 4-1) that a PWR has a higher propensity for vapor pull through due to the vortex flow then either LOFT or Semiscale.

2) No experimental data were found in the literature on vapor pull-through in a vortex free flow for conditions of interest to a PWR. However, experimental data and correlations are available (see Equations 4-10 and 4-11) for vortex free pull-through drains in large vessels.

An application of these correlations to a PWR, LOFT and Semiscale indicates that conditions which may lead to an incipient vortex free vapor pull-through in a PWR are bracketted by those scaled to LOFT and Semiscale (see Table 4-2). Furthermore, these results indicate also a considerable propensity for vapor pull through a small break in a PWR (see Equation 4-19).

6.4 CCFL in Horizontal Pipes

1. Experimental data on CCFL phenomena in horizontal pipes, applicable to PWR conditions were not be found in the literature. However, some data are available on air-water flooding in a rectangular horizontal channel.

   An application of the proposed correlation (see Equation 5-1) indicates that conditions which may lead to CCFL in a PWR are bracketted by those scaled to LOFT and Semiscale (see Figure 5-2). These results also indicate a potential for CCFL phenomena occurring in a hot leg of a PWR.

2. Available correlations (see Equation 5-5) for calculating the length of an arrested liquid wedge (see Figure 5-1) shows that this length is a strong function of the velocity of the lighter phase. When applied to a PWR, LOFT, and Semiscale the correlation indicates that the condition for arresting an advancing liquid wedge in a hot leg of a PWR is bounded by those scaled to LOFT and Semiscale (see Table 5-1).

6.5 State of Fluid Reaching the Break

The data base of correlations used in this report does not correspond to PWR conditions. Consequently, definitive quantitative statements on the precise state of the fluid reaching the break cannot be made. Nevertheless, the results indicate that due to flow regime transitions and/or liquid entrainment and/or vapor pull-through there is a great propensity for a two phase mixture reaching the break during most of the transient.

References

1. Ybarrondo, L. Y., Griffith, P., Fabic, S and G. D. McPherson, "Examination of LOFT Scaling," ASME Paper 74-WA/HT-53, ASME Annual Winter Meeting New York (1974).

2. Carbiener W. A. and R. A. Chudnik, "Similitude Considerations for Modeling Nuclear Reactor Blowdowns," Trans. Am. Nucl. Soc., Vol. 12, 361, (1969).

3. Nahavandi, A.N., Castellana, F. S. and E. A. Moradkhanian, "Scaling Laws for Modeling Nuclear Reactor Systems," Nucl. Sc and Engr., Vol. 72, 75, (1979).

4. Birkhoff, G. "Hydrodynamics - a Study in Logic, Fact and Similitude," Dover Publ. Inc., New York, NY, (1950).

5. Taitel, Y., and A. E. Dukler, "A Model for Predicting Flow Regime Transitions in Horizontal and Near Horizontal Gas-Liquid Flow," AIChE Journal, Vol. 22, 47, (1976).

6. Taitel, Y. Lee, N. and A. E. Dukler, "Transient Gas-Liquid Flow in Horizontal Pipes: Modeling The Flow Regime Transitions," AIChE Journal, Vol. 24, 920 (1978).

7. Craya, A., "Theoretical Research on the Flow of Non-Homogeneous Fluids," La Houille Blanche, pg. 44-55, January-February 1949.

8. Gariel, P., "Experimental Research on the Flow of Non-Homogeneous Fluids," La Houille Blanche, pg. 56-64, January-February 1949.

9. Rouse, H., "Seven Exploratory Studies in Hydraulics," Proc. ASCE, Vol. 82, (1956).

10. Daggett, L. and G. Keulegan, "Similitude in Free Surface Vortex Formation," J. Hydr. Div. ASCE, Vol. 100, 1506, (1974).

11. Plesset, M.S., "Remarks on Similitude Scaling of Vortex Motion in Draining Liquids," Internal Memorandum Report, General Dynamics Corp., San Diego, California, April 1957.

12. Lubin, B., and M. Hurwitz, "Vapor Pull-Through at a Tank Drain - with and without Dielectrophoretic Buffling," Proc. Conf. Long Term Cryo-Propellant Storage in Space, NASA Mrshall Space Center, Huntsville, Ala., pg. 173, October 1966.

13. Wallis, G. B., "Flooding in Stratified Gas-Liquid Flow," Dartmouth College Report No. 27327-9, August 1970.

14. Karman, Th. von, "The Engineer Grapples with Nonlinear Problems," Bul. Am. Math. Soc., Vol. 46, 615 (1940).

15. Keulegan, G., "Form Characteristics of Arrested Saline Wedges," Nat. Bur. Stand. Report 5482, Washington D.C., October 4, 1957.

16. Grubert, F. P., "Experiments on Arrested Saline Wedge," J. Hydr. Div. ASCE, Vol. 108, 945, (1980).

Appendix A

Geometric Similarty for Separated Two-Phase Flow

Using the notation shown in Fig. A-1, the geometric relations of interest to separated two phase flow, can be expressed in terms of D, θ and β, thus one obtains:

a) for the cross-sectional area occupied by the vapor:

$$A_g = \frac{D^2}{4} [\theta - \sin\theta \cos\theta] \quad \text{A-1}$$

b) for the void fraction:

$$\alpha = \frac{1}{\Pi} [\theta - \sin\theta \cos\theta] \quad \text{A-2}$$

c) for the three perimeters in dimensionless form:

$$\frac{\xi_i}{D} = \sin\theta \quad \text{A-3}$$

$$\frac{\xi_{gw}}{D} = \theta \quad \text{A-4}$$

$$\frac{\xi_{lw}}{D} = \Pi - \theta \quad \text{A-5}$$

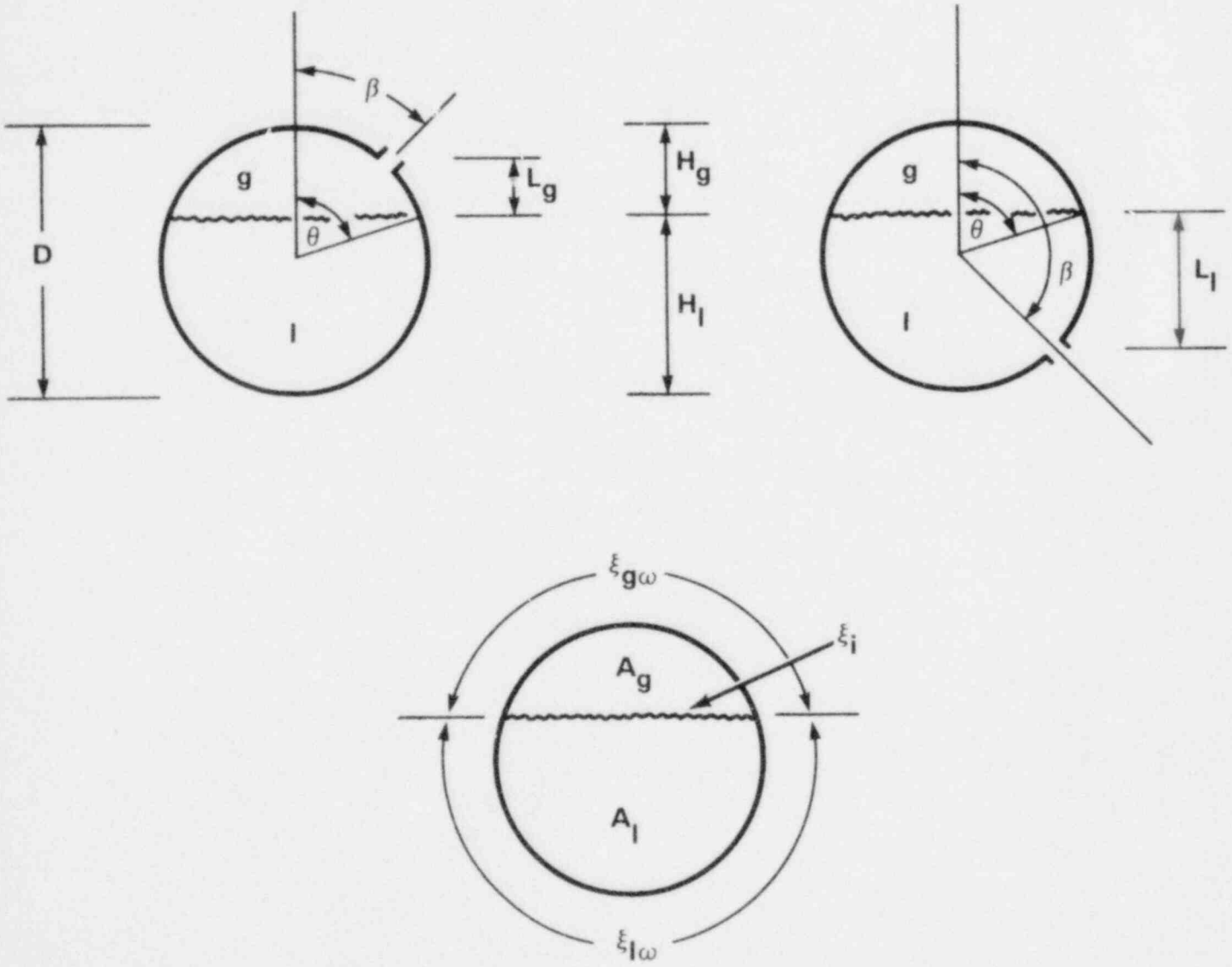

FIG. A-1 DEFINITION OF NOTATIONS

d) for the dimensionless depths of the liquid:

$$\frac{H_\ell}{D} = \frac{1}{2} (1 + \cos \theta) \qquad \text{A-6}$$

and of the vapor

$$\frac{H_g}{D} = \frac{1}{2} (1 - \cos \theta) \qquad \text{A-7}$$

e) for the dimensionless distances from the break

$$\frac{L_g}{D} = \frac{1}{2} [\cos \beta - \cos \theta) \qquad \text{A-8}$$

and

$$\frac{L_\ell}{D} = \frac{1}{2} [\cos \theta - \cos \beta) \qquad \text{A-9}$$

Geometric similarity between model and prototype requires that

$$\theta_m = \theta_p \qquad \text{A-10}$$

and

$$\beta_m = \beta_p \qquad \text{A-11}$$

It follows then from Eq. A-2 through Eq. A-9, that the following relations are automatically satisfied:

$$\alpha_m = \alpha_p \tag{A-12}$$

$$\left(\frac{\xi_i}{D}\right)_m = \left(\frac{\xi_i}{D}\right)_p \tag{A-13}$$

$$\left(\frac{\xi_{gw}}{D}\right)_m = \left(\frac{\xi_{gw}}{D}\right)_p \tag{A-14}$$

$$\left(\frac{\xi_{\ell w}}{D}\right)_m = \left(\frac{\xi_{\ell w}}{D}\right)_p \tag{A-15}$$

$$\left(\frac{H_\ell}{D}\right)_m = \left(\frac{H_\ell}{D}\right)_p \tag{A-16}$$

$$\left(\frac{H_g}{D}\right)_m = \left(\frac{H_g}{D}\right)_p \tag{A-17}$$

$$\left(\frac{L_g}{D}\right)_m = \left(\frac{L_g}{D}\right)_p \tag{A-18}$$

$$\left(\frac{L_\ell}{D}\right)_m = \left(\frac{L_\ell}{D}\right)_p \tag{A-19}$$

We conclude therefore, that in separated two-phase flow, geometric similarity implies the equality of void fractions and vice versa.

We note also that instead of θ, one could have selected for the independent variable any of the other geometric relations say, for example, H_ℓ/D. In this case the void fraciton becomes

$$\alpha = \frac{1}{\pi}\left\{ \cos^{-1}\left(\frac{2H_\ell}{D} - 1\right) - \left(\frac{2H_\ell}{D} - 1\right)\sqrt{1-\left(\frac{H_\ell}{D} - 1\right)^2}\right\} \qquad \text{A-20}$$

which is plotted in Figure A-2.

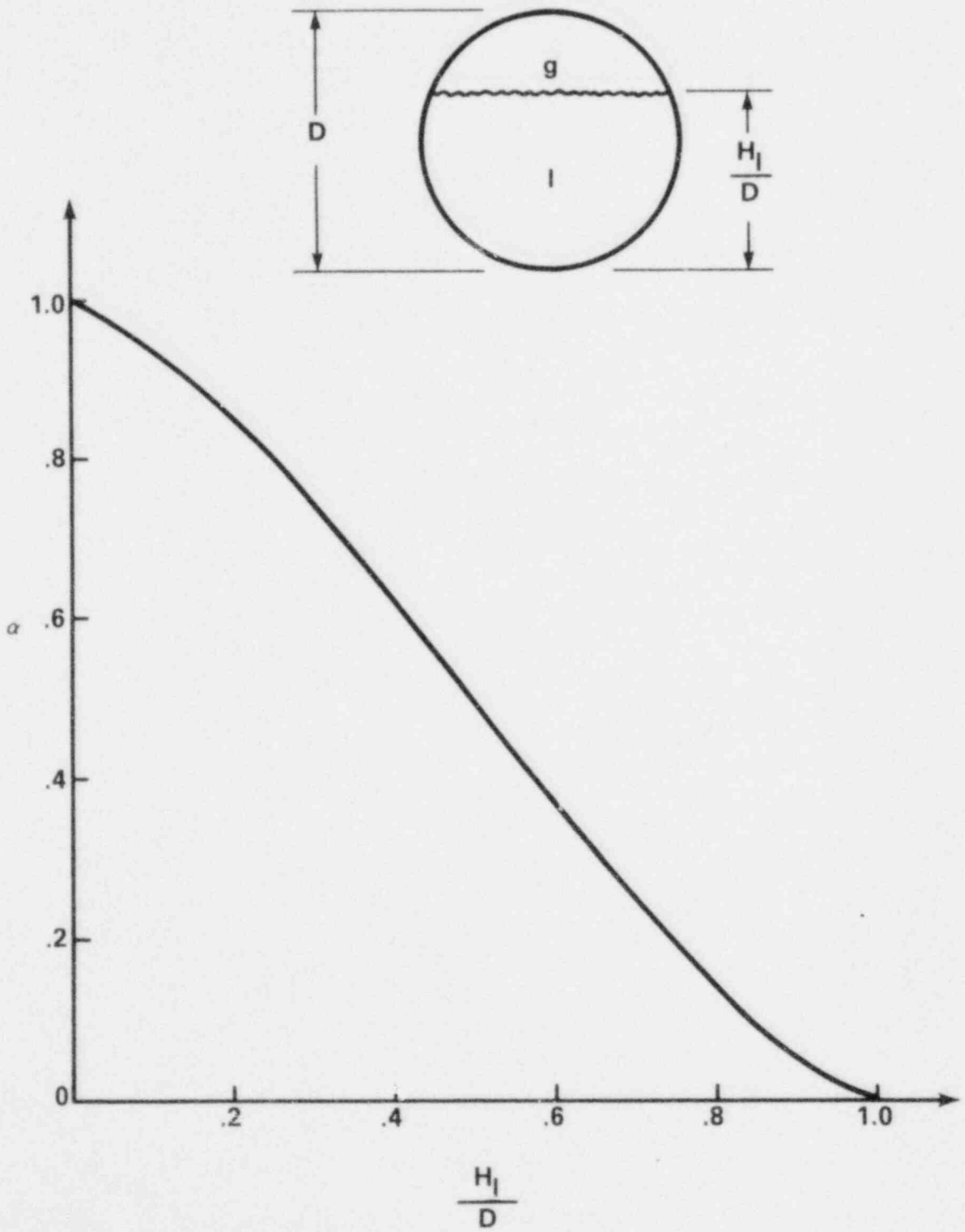

FIG. A-2 RELATION BETWEEN VOID FRACTION AND LIQUID DEPTH

Appendix B

Power to Volume Scaling

B.1 Requirements and Implications

In this section we shall discuss the power to volume scaling method together with its requirements and implications.* This is being done here in order to compare this approach to the scaling of separated two-phase flow through horizontal pipes. This latter analysis is carried out in Appendix C.

For single phase, one-dimensional vertical flow, the equations which describe the conservation of mass, momentum and of energy are:

$$\frac{\partial \rho}{\partial t} + \frac{\partial}{\partial z}\rho v = 0 \qquad \text{B-1}$$

$$\rho \frac{\partial v}{\partial t} + \rho v \frac{\partial v}{\partial z} = -\frac{\partial P}{\partial z} - \frac{\Sigma_w \tau}{A_c} - g\rho \qquad \text{B-2}$$

$$\rho \frac{\partial h}{\partial t} + \rho v \frac{\partial h}{\partial z} = \frac{\Sigma q}{A_c} + \frac{\partial P}{\partial t} + v \frac{\partial P}{\partial z} \qquad \text{B-3}$$

*For additional information and applications to experimental facilities, the reader is referred to Ref. 1 through Ref. 3.

It is noted that these equations are also applicable to two-phase flow under the assumption that the two phases have equal velocities and temperatures. Introducting the following dimensionless parameters

$$t^+ = \frac{t}{t_o} \;,\quad z^+ = \frac{z}{l_o} \;,\quad \rho^+ = \frac{\rho}{\rho_o} \;,\quad v^+ = \frac{v}{v_o} \;,\quad p^+ = \frac{p}{p_o} \qquad \text{B-4}$$

$$\tau^+ = \frac{\tau}{\kappa \rho_o v_o^2} \;,\quad h^+ = \frac{h}{h_o} \;,\quad q^+ = \frac{q}{q_o} \;,\quad \xi^+ = \frac{\xi}{\xi_o} \;,\quad A_c^+ = \frac{A}{A_o}$$

where the subscript zero, denotes the reference scale, Eq. B-1 through Eq. B-3 can be expressed in dimensionless form, thus

$$\frac{\partial \rho^+}{\partial t^+} + \left[\frac{v_o t_o}{l_o}\right] \frac{\partial \rho^+ v^+}{\partial z^+} = 0 \qquad \text{B-5}$$

$$\rho^+ \frac{\partial v^+}{\partial t^+} + \left[\frac{v_o t_o}{l_o}\right] \rho^+ v^+ \frac{\partial v^+}{\partial z^+} = -\left[\frac{p_o}{l_o}\,\frac{t_o}{\rho_o v_o}\right] \frac{\partial p^+}{\partial z^+} - \left[\frac{\xi_o}{A_{co}} K v_o t_o\right] \frac{\xi^+}{A_c^+} \tau^+ - \left[\frac{g t_o}{v_o}\right] \rho^+ \qquad \text{B-6}$$

$$\rho^+ \frac{\partial h^+}{\partial t^+} + \left[\frac{v_o t_o}{l_o}\right] \rho^+ v^+ \frac{\partial h^+}{\partial z^+} = \left[\frac{\xi_o}{A_{co}}\,\frac{q_o t_o}{\rho_o h_o}\right] \frac{\xi^+}{A^+} q^+ + \qquad \text{B-7}$$

$$+ \left[\frac{p_o}{\rho_o h_o}\right] \frac{\partial p^+}{\partial t^+} + \left[\frac{v_o t_o}{l_o}\,\frac{p_o}{\rho_o h_o}\right] v^+ \frac{\partial p^+}{\partial z^+}$$

Consequently, if the similarity is to be achieved between processes observed in a model and in the prototype, it is necessary to satisfy the following identities

$$\left[\frac{vt}{l}\right]_m = \left[\frac{vt}{l}\right]_p \qquad \text{B-8}$$

$$\left[\frac{p}{\rho}\,\frac{t}{lv}\right]_m = \left[\frac{p}{\rho}\,\frac{t}{lv}\right]_p \qquad \text{B-9}$$

$$\left[\frac{\Sigma}{A_c}\,Kvt\right]_m = \left[\frac{\Sigma}{A_c}\,Kvt\right]_p \qquad \text{B-10}$$

$$\left[\frac{gt}{v}\right]_m = \left[\frac{gt}{v}\right]_p \qquad \text{B-11}$$

$$\left[\frac{\Sigma}{A_c}\,\frac{qt}{\rho h}\right]_m = \left[\frac{\Sigma}{A_c}\,\frac{qt}{\rho h}\right]_p \qquad \text{B-12}$$

$$\left[\frac{p}{\rho h}\right]_m = \left[\frac{p}{\rho h}\right]_p \qquad \text{B-13}$$

where for simplicity, we have omitted the subscript zero. Let us examine now the implications of these identities.

The dimensionless group which appears in the mass conservation equation, Eq. B-5, is referred to in the literature as the Strouhal number. Referring now to Eq. B-6 and Eq. B-7, it can be seen that this number scales also the fluxes of momentum and of enthalpy. Conseqeuntly, if a model and prototype have equal Strouhal numbers, then the rates of change of mass, momentum and of enthalpy (given by the left hand sides of Eq. B-5, Eq. B-6 and Eq. B-7) in the two systems will be similar. It is evident that when these rates of change are high (such as in a case of a large LOCA), the equality of Strouhal numbers must be maintained.

If the model and prototype have the same fluid and the processes occur at the same pressure, Eq. B-13 is satisfied. With Strouhal numbers being equal, Eq. B-7 then indicates that the rate of pressure change will have a similar effect on the energy content of the two systems. It is evident that if the effects of decompression and/or recompression are to be scaled, then both Eq. B-8 and Eq. B-13 must be satisfied.

The effect of wall heat flux is scaled by Eq. B-12. If we require that the events in model and prototype occur at the same time, then with pressures being equal, Eq. B-12 reduces to

$$\left[\frac{\Sigma q}{A_c}\right]_m = \left[\frac{\Sigma q}{A_c}\right]_p$$

Defining the total volume and power of the system by

$$\mathcal{V} = \ell A_c \qquad \text{B-15}$$

and

$$\Phi = \ell \xi q \qquad \text{B-16}$$

Eq. B-14 can be expressed also as

$$\frac{\Phi_p}{\Phi_m} = \frac{\mathcal{V}_p}{\mathcal{V}_m} \qquad \text{B-17}$$

Furthermore, when the time scale is preserved, that is, for isochronous events in model and prototype, the equality of Strouhal numbers, Eq. B-8, reduces to

$$\left(\frac{v}{\ell}\right)_m = \left(\frac{v}{\ell}\right)_p \qquad \text{B-18}$$

Defining the volumetric flow rate by

$$Q = vA_c \qquad \text{B-19}$$

then in view of Eq. B-15, we obtain from Eq. B-18 and Eq. B-19 the ratio of volumetric flow rates

$$\frac{Q_p}{Q_m} = \frac{\mathcal{V}_p}{\mathcal{V}_m} \qquad \text{B-20}$$

Since the processes take place at the same pressure and with the same fluid Eq. B-10 can be expressed also as

$$\frac{W_p}{W_m} = \frac{\vartheta_p}{\vartheta_m} \qquad \text{B-21}$$

It follows then from Eq. B-17, Eq. B-20 and Eq. B-21 that

$$\frac{\phi_p}{\phi_m} = \frac{W_p}{W_m} = \frac{Q_p}{Q_m} = \frac{\vartheta_p}{\vartheta_m} = S \qquad \text{B-22}$$

which expresses the power to volume scaling relations.

We note, that when Eq. B-22 is satisfied there is a one to one relation between the corresponding terms of the mass and energy conservation equations for model and for prototype. In other words, in going from model to prototype the effects of various process accounted for in Eq. B-5 and Eq. B-7 are preserved without distortion.

Satisfying the similarity conditions for mass and energy conservation with Eq. B-22, it remains to establish the requirements for scaling the effects of pressure, friction and gravity in the momentum equation, Eq. B-6. Note, that the effect of inertia has been already accounted for (scaled) by the equality of Strouhal numbers, Eq. B-8.

For pressure, friction and gravity to have a similar effect in model and prototype, Eq. B-9 through Eq. B-11 must be satisfied. Since the requirements

of isochronicity and of equal properties have been already invoked, these three equations reduce respectively to

$$\frac{(v\ell)m}{(v\ell)p} = \Delta_1 \qquad \text{B-23}$$

$$\frac{v_m}{v_p} = \Delta_2 \qquad \text{B-24}$$

$$\left[\frac{\xi}{A_c} Kv\right]_m = \Delta_3 \left[\frac{\xi}{A_c} Kv\right]_p \qquad \text{B-25}$$

If the effects of pressure, gravity and friction are to be identical in the model and prototype, then the values of the distortion coefficients Δ_1, Δ_2 and Δ_3, should be equal to unity. Eq. B-23 and Eq. B-24 are two relations for scaling velocities and lengths. However, a third relation was already specified by the equality of Strouhal numbers which for isochronous events reduces to Eq. B-18. In order to satisfy simultaneously, these three relations, it is necessary to preserve elevations and velocities between model and prototype, that is,

$$\frac{\ell_p}{\ell_m} = 1 \qquad \text{B-26}$$

and

$$\frac{v_p}{v_m} = 1 \qquad \text{B-27}$$

The requirement of equal elevations imposes in turn, a requirement for scaling cross sectional areas which is obtained from Eq. B-15 and Eq. B-26, thus

$$\frac{A_{cp}}{A_{cm}} = \frac{\vartheta_p}{\vartheta_m} = S \qquad \text{B-28}$$

The requirement for scaling the effect of frictional forces, Eq. B-25, then becomes

$$\left[\frac{\xi}{\vartheta} K\right]_m = \left[\frac{\xi}{\vartheta} K\right]_p \qquad \text{B-29}$$

To summarize, the effects of each of the terms appearing in the three conservation equations are preserved in model and prototype without any distortion, if one satisfies the requirements of:

a) Equal pressures and properties:

$$\frac{\gamma_p}{\gamma_m} = \frac{\rho_p}{\rho_m} = \frac{h_p}{h_m} = 1 \qquad \text{B-30}$$

b) Power to volume scaling relations:

$$\frac{\Phi_p}{\Phi_m} = \frac{W_p}{W_m} = \frac{Q_p}{Q_m} = \frac{q}{v_m} = S \qquad \text{B-31}$$

which imply isochronicity:

$$\frac{t_p}{t_m} = 1 \qquad \text{B-32}$$

c) Equal elevations

$$\frac{l_p}{l_m} = 1 \qquad \text{B-33}$$

which together with Eq. B-31, specifies the ratio of cross sectional areas given by Eq. B-28. Note, that Eq. B-33 and Eq. B-32 imply also equal velocities, Eq. B-27.

d) Equal frictional effects:

$$\left[\frac{\Sigma}{A_c} K\right]_m = \left[\frac{\Sigma}{A_c} K\right]_p \qquad \text{B-34}$$

If some of these requirements are not satisfied, then the effects of some of the processes observed in model and prototype will be distorted.

B.2 Applications

We want to determine the volumetric flow rates of the vapor, that satisfy the power to volume scaling. We can easily obtain such an expression if we assume that the effect of pressure decrease on vapor formation is small when compared to that of the decay heat. This is a reasonable approximation for slow decompression rates associated with small breaks. The vapor flow rates are obtained then from an overall energy balance, that is, from

$$\phi = \rho_g \, h_{fg} \, Q_g \qquad \text{B-35}$$

Since the vapor superficial velocity j_g, is related to Q_g by

$$j_g = \frac{Q_g}{A_c} \qquad \text{B-36}$$

It follows then from Eq. B-35 and Eq. B-36 that

$$j_g = \frac{\phi}{\rho_g \, h_{fg} \, A_c} \qquad \text{B-37}$$

whence

$$\frac{j_{gm}}{j_{gp}} = \left(\frac{\Phi}{A_c}\right)_m \left(\frac{A_c}{\phi}\right)_p = \frac{1}{S} \left(\frac{D_p}{D_m}\right)^2 \qquad \text{B-38}$$

where S is the plant to model power ratio

$$S = \frac{\phi_p}{\phi_m} \qquad \text{B-39}$$

These are the relations which were used in the body of the report.

In order to relate S to the break size, we note that volumetric flow rates scale according to

$$S = \frac{Q_{gp}}{Q_{gm}} = \frac{v_p}{v_m}\left(\frac{d_p}{d_m}\right)^2 \qquad \text{B-40}$$

assuming that the flow of the break is choked then

$$v_p = v_m \qquad \text{B-41}$$

and Eq. B-40 reduces to

$$S = \left(\frac{d_p}{d_m}\right)^2 \qquad \text{B-42}$$

which was also used in the preceeding sections of this report.

Appendix C

Two Fluid Model Scaling of Separated Flow through Horizontal Pipes

C.1 Formulation

In this section we shall examine the rules for scaling separated two-phase flow in horizontal ducts using the two fluid model. We shall assume the phases to be in thermodynamic equilibrium, flowing adiabatically and consider small break phenomena for which the rate of depressurization is slow. Consequently, we can omit the two energy equations and formulate the problem in terms of the mass conservation equations

$$\frac{\partial}{\partial}[(1-\alpha)\rho_\ell] + \frac{\partial}{\partial z}[(1-\alpha)\rho_\ell v_\ell] = 0 \qquad C-1$$

$$\frac{\partial}{\partial t}[\alpha\rho_g] + \frac{\partial}{\partial z}[\alpha\rho_g v_g] = 0 \qquad C-2$$

and the momentum conservation equations

$$A_\ell \rho_\ell \frac{\partial v_\ell}{\partial t} + A_\ell \rho_\ell v_\ell \frac{\partial v_\ell}{\partial z} = -\frac{\partial[A_\ell P_\ell]}{\partial z} + P_{\ell i}\frac{\partial A_\ell}{\partial z} - \tau_{\ell w}\xi_{\ell w} + \tau_i \xi_i \qquad C-3$$

$$A_g \rho_g \frac{\partial v_g}{\partial t} + A_g \rho_g v_g \frac{\partial v_g}{\partial z} = -\frac{\partial[A_g P_g]}{\partial z} + P_{gi}\frac{\partial A_g}{\partial z} - \tau_{gw}\xi_{gw} - \tau_i \xi_i \qquad C-4$$

where the variables are area averaged.* Note, that the pressures P_ℓ and P_g

*A detailed derivation and discussion of area averaged equations for the two-fluid model can be found in the PhD dissertation: "Thermo-Fluid Dynamics of Separated Two-Phased Flow," by G. Kocamustafaoguari, Georgia Institute of Technology, Dec. 1971

are not equal because of the hydrostatic effect. Following the "hydraulic" approximation they can be obtained from the transvers momentum equations when the inertia terms are neglected thus

$$P_\ell = P_{\ell i} + \frac{1}{2} \rho_\ell g H_\ell \qquad C-5$$

and

$$P_g = P_{gi} - \frac{1}{2} \rho_g g H_g \qquad C-6$$

where P_{gi} and $P_{\ell i}$ are the pressures just above and below the interface. If we neglect the effect of surface tension then

$$P_{gi} = P_{\ell i} \qquad C-7$$

Substituting Eq. C-5 and Eq. C-6 into Eq. C-3 and Eq. C-4 and expressing them in terms of the void fraction we obtain

$$\rho_\ell \frac{\partial v_\ell}{\partial t} + \rho_\ell v_\ell \frac{\partial v_\ell}{\partial z} = -\frac{\partial P_\ell}{\partial z} - \frac{g \rho_\ell H_\ell}{2(1-\alpha)} \frac{\partial (1-\alpha)}{\partial z} + \frac{\tau_i \xi_i}{A_c (1-\alpha)} - \frac{\tau_{\ell w} \xi_{\ell w}}{A_c (1-\alpha)} \qquad C-8$$

$$\rho_g \frac{\partial v_g}{\partial t} + \rho_g v_g \frac{\partial v_g}{\partial z} = -\frac{\partial P_g}{\partial z} + \frac{g \rho_g H_g}{2 \alpha} \frac{\partial \alpha}{\partial z} - \frac{\tau_i \xi_i}{A_c \alpha} - \frac{\tau_{gw} \xi_{gw}}{A_c \alpha} \qquad C-9$$

Two comments should be made with respect to these equations. First, the void fraction gradient terms which appear in Eq. C-8 and Eq. C-9, make these equations hyperbolic, that is, they make the problem "well posed." Secondly, these two terms account for the effect of gravity in horizontal flow. Were it not for them, the equations could not model gravity dominated flows of interest here.

The four equations, that is, Eq. C-1, C-2, C-8, and C-9, describe the two fluid model for separated horizontal flow. In the section that follows, they will be used to obtain the scaling relations appropriate to this two-phase flow regime.

C-2 Scaling Requirements

Introducing the following dimensionless parameters for the liquid phase:

$$A_\ell^+ = \frac{A_\ell}{A_{\ell o}}\,,\quad t^+ = \frac{t}{t_o}\,,\quad z^+ = \frac{z}{\ell_o}\,,\quad (1-\alpha)^+ = \frac{1-\alpha}{1-\alpha_o}\,,$$

$$\rho_\ell^+ = \frac{\rho_\ell}{\rho_{\ell o}}\,,\quad v_\ell^+ = \frac{v_\ell}{v_{\ell o}}\,,\quad P_\ell^+ = \frac{P_\ell}{P_{\ell o}}\,,\quad v_r^+ = \frac{v_g - v_\ell}{v_{go} - v_{\ell o}}$$

$$H_\ell^+ = \frac{H_\ell}{H_{\ell o}}\,,\quad \xi_i^+ = \frac{\xi_i}{\xi_{io}}\,,\quad \xi_{\ell w}^+ = \frac{\xi_{\ell w}}{\xi_{\ell w o}}\,, \qquad \text{C-10}$$

$$\tau_{\ell w}^+ = \frac{\tau_{\ell w}}{K_\ell \rho_{\ell o} v_{\ell o}^2}\,,\quad \tau_i^+ = \frac{\tau_i}{C_D \rho_{go} (v_{go} - v_{\ell o})^2}$$

with a similar set for the vapor phase, we can express the four conservation equations in dimensionless form thus:

$$\frac{\partial}{\partial t^+}\left[(1-\alpha)^+\rho_\ell^+\right] + \left[\frac{v_{\ell o}\, t_o}{l_o}\right]\frac{\partial}{\partial z^+}\left[(1-\alpha)^+\rho_\ell^+ v_\ell^+\right] = 0 \qquad C-11$$

$$\frac{\partial}{\partial t^+}\left[\alpha^+\rho_g^+\right] + \left[\frac{v_{go}\, t_o}{l_o}\right]\frac{\partial}{\partial z^+}\left[\alpha^+\rho_g^+ v_g^+\right] = 0 \qquad C-12$$

$$\rho_\ell^+\frac{\partial v_\ell^+}{\partial t^+} + \left[\frac{v_{\ell o}\, t_o}{l_o}\right]\rho_\ell^+ v_\ell^+\frac{\partial v_\ell^+}{\partial z^+} =$$

$$= -\left[\frac{P_{\ell o}}{\rho_{\ell o}}\frac{t_o}{l_o v_{\ell o}}\right]\frac{\partial P^+}{\partial z^+} - \left[\frac{g\, t_o}{v_{\ell o}}\frac{H_{\ell o}}{l_o}\right]\frac{H_\ell^+}{2(1-\alpha)^+}\frac{\partial(1-\alpha)^+}{\partial z^+} + \qquad C-$$

$$+ \left[C_D\frac{\rho_{go}\, v_{ro}^2}{\rho_{\ell o}\, v_{\ell o}}\frac{t_o}{(1-\alpha)_o}\frac{\xi_{io}}{A_{co}}\right]\frac{\tau_i^+\xi_i^+}{(1-\alpha)^+ A_c^+} - \left[K_\ell\frac{v_{\ell o}\, t_o}{(1-\alpha)_o}\frac{\xi_{\ell w o}}{A_{co}}\right]\frac{\tau_{\ell w}^+\xi_{\ell w}^+}{(1-\alpha)^+ A_c^+}$$

$$\rho_g^+\frac{\partial v_g^+}{\partial t^+} + \left[\frac{v_{go}\, t_o}{l_o}\right]\rho_g^+ v_g^+\frac{\partial v_g^+}{\partial z^+} =$$

$$= -\left[\frac{P_{go}}{\rho_{go}}\frac{t_o}{l_o v_{go}}\right]\frac{\partial P_g^+}{\partial z^+} + \left[\frac{g\, t_o}{v_{go}}\frac{H_{go}}{l_o}\right]\frac{H_g^+}{2\alpha^+}\frac{\partial\alpha^+}{\partial z^+} - \qquad C-1$$

$$- \left[C_D\frac{v_{ro}^2}{v_{go}}\frac{t_o}{\alpha_o}\frac{\xi_{io}}{A_{co}}\right]\frac{\tau_i^+\xi_i^+}{\alpha^+ A_c^+} - \left[K_g\frac{v_{go}\, t_o}{\alpha_o}\frac{\xi_{gwo}}{A_{co}}\right]\frac{\tau_{gw}^+}{\alpha^+}\frac{\xi_{gw}^+}{A_c^+}$$

Similarity between model and prototype requires equality of corresponding dimensionless groups. If we assume geometric similarity and equal properties this implies the following equalities for the liquid phase;

$$\left[\frac{v_{\ell_o} t_o}{l_o}\right]_m = \left[\frac{v_{\ell_o} t_o}{l_o}\right]_p \qquad C-15$$

$$\left[\frac{t_o}{l_o v_{\ell_o}}\right]_m = \left[\frac{t_o}{l_o v_{\ell_o}}\right]_p \qquad C-16$$

$$\left[\frac{g t_o}{v_{\ell_o}} \frac{D_o}{l_o}\right]_m = \left[\frac{g t_o}{v_{\ell_o}} \frac{D_o}{l_o}\right]_p \qquad C-17$$

$$\left[K_\ell \frac{v_{\ell_o} t_o}{l_o} \frac{l_o}{D_o}\right]_m = \left[K_\ell \frac{v_{\ell_o} t_o}{l_o} \frac{l_o}{D_o}\right]_p \qquad C-18$$

and for the vapor;

$$\left[\frac{v_{g_o} t_o}{l_o}\right]_m = \left[\frac{v_{g_o} t_o}{l_o}\right]_p \qquad C-19$$

$$\left[\frac{t_o}{l_o v_{g_o}}\right]_m = \left[\frac{t_o}{l_o v_{g_o}}\right]_p \qquad C-20$$

$$\left[\frac{g t_o}{v_{g_o}} \frac{D_o}{l_o}\right]_m = \left[\frac{g t_o}{v_{g_o}} \frac{D_o}{l_o}\right]_p \qquad C-21$$

$$\left[K_g \frac{v_{g_o} t_o}{l_o} \frac{l_o}{D_o}\right]_m = \left[K_g \frac{v_{g_o} t_o}{l_o} \frac{l_o}{D_o}\right]_p \qquad C-22$$

These two sets are coupled through the two equalities which scale the momentum exchange at the interface between the phases, that is, for the liquid:

$$\left[C_D \left(\frac{v_{r_0}}{v_{l_0}} \right)^2 \frac{v_{l_0} t_0}{l_0} \frac{l_0}{D_0} \right]_m = \left[C_D \left(\frac{v_{r_0}}{v_{l_0}} \right)^2 \frac{v_{l_0} t_0}{l_0} \frac{l_0}{D_0} \right]_p \qquad C-22$$

and for the vapor

$$\left[C_D \left(\frac{v_{r_0}}{v_{g_0}} \right)^2 \frac{v_{g_0} t_0}{l_0} \frac{l_0}{D_0} \right]_m = \left[C_D \left(\frac{v_{r_0}}{v_{g_0}} \right)^2 \frac{v_{g_0} t_0}{l_0} \frac{l_0}{D_0} \right]_p \qquad C-23$$

Comparing the similarity requirements for a two fluid model, that is, Eq. C-15 through Eq. C-21, with those for the homogeneous flow model, that is, Eq. B-8 through Eq. B-11, it can be seen that not only the number of equalities has been doubled, but that two additional relations, Eq. C-22, and Eq. C-23, have appeared to account for interfacial momentum exchange.

The problem can be made tractable by noticing that the scales of time t_0, and of length l_0, which appear in the liquid and vapor sets of equations are the same. Consequently, they can be eliminated from the corresponding equalities in the two sets. For example, from Eq. C-15, and Eq. C-19 we obtain the similarity requirement

$$\left[\frac{v_{g_0}}{v_{l_0}} \right]_m = \left[\frac{v_{g_0}}{v_{l_0}} \right]_p \qquad C-24$$

The same requirement is obtained from Eq. C-16 and Eq. C-20, Eq. C-17 and Eq. C-20, Eq. C-22, and Eq. C-23, whereas Eq. C-18 and Eq. C-21 yield

$$\left[\frac{K_g}{K_\ell}\right]_m = \left[\frac{K_g}{K_\ell}\right]_p \qquad C-25$$

Let us examine now the implications of these requirements.

Eq. C-24 states that the slip ratio in the model and in the prototype must be equal. Since we have already invoked geometric similarity, that is, equality of void fraction.

$$\alpha_m = \alpha_p \qquad C-26$$

Eq. C-24 implies that

$$\left[\frac{j_{g0}}{j_{\ell 0}}\right]_m = \left[\frac{j_{g0}}{j_{\ell 0}}\right]_p \qquad C-27$$

Consequently for similarity, the model and the prototype must have the same ratio of superficial velocities.

Eq. C-25 states that the model and prototype must have the same ratio of friction factors. Now, available correlations, for example that of Martineli and coworkers, show that for a given fluid and flow regime, this ratio depends only on the ratio of superficial velocities. Consequently, if Eq. C-27 is satisfied so will be Eq. C-25.

We conclude, therefore, that if Eq. C-26 and Eq. C-27 are satisfied, then one needs to consider the set of equalities for one phase only (say Eq. C-15 through Eq. C-18) and one coupling equality (say Eq. C-22). The five equalities pertaining to the other phase are then satisfied automatically.

Let us consider the equalities pertaining to the liquid phase, that is, Eq. C-15 through Eq. C-18 and the interfacial momentum coupling equation Eq. C-22. It will be instructive to compare this set to the corresponding one valid for the homogeneous model, that is, to Eq. B-8, B-9, B-10 and B-11. It can be seen that the Strouhal number equality appears in both sets. Secondly, the terms which scale the pressure and the wall friction are of the same form. However, these two sets differ in the groups that scale the effect of gravity. Note that Eq. C-17 has an D_o/l_o term which does not appear in Eq. B-11. It will be seen that because of this difference, the two sets obey different scaling rules.

Following the same reasoning as in Appendix B, we shall require first the equality of Strouhal numbers:

$$\left[\frac{v_{\ell_o} t_o}{l_o}\right]_m = \left[\frac{v_{\ell_o} t_o}{l_o}\right]_p \qquad C-28$$

Since the flows are gravity dominated, we want to account properly for the effects of gravity. Consequently, we want to satisfy also

$$\left[\frac{g t_o}{v_{lo}} \frac{D_o}{l_o}\right]_m = \left[\frac{g t_o}{v_{lo}} \frac{D_o}{l_o}\right]_p \qquad C-29$$

We observe now that if both equations, that is, Eq. C-28 and Eq. C-29, are to be satisfied, we cannot preserve the scale of time unless

$$\left[\frac{l^2}{D}\right]_m = \left[\frac{l^2}{D}\right]_p \qquad C-30$$

However, Eq. C-28 and Eq. C-29, can be satisfied simultaneously, if the velocity scales according to

$$v \sim \sqrt{gD} \qquad C-31$$

so that these two equations reduce to one requirement for scaling time,

$$\left[\frac{t_o\sqrt{D_o}}{l_o}\right]_m = \left[\frac{t_o\sqrt{D_o}}{l_o}\right]_p \qquad C-32$$

and a second one which scales the velocities:

$$\frac{v_m}{v_p} = \sqrt{\frac{D_m}{D_p}} \qquad C-33$$

We conclude therefore, that if Eq. C-33 and Eq. C-32 are satisfied, then the

effects of mass flux, of mementum flux and of gravity will be preserved in scaling from model to prototype.

Consider now the equalities that scale the effects of pressure, Eq. C-16, of wall friction Eq. C-17 and of interfacial drag Eq. C-22 which in view of Eq. C24, and Eq. C-28 and Eq. C-33 reduce respectively to

$$\left[\frac{t_o}{\ell_o\sqrt{D_o}}\right]_m = \left[\frac{t_o}{\ell_o\sqrt{D_o}}\right]_P \qquad C-34$$

$$\left[K_\ell \frac{\ell_o}{D_o}\right]_m = \left[K_\ell \frac{\ell_o}{D_o}\right]_P \qquad C-35$$

$$\left[C_D \frac{\ell_o}{D_o}\right]_m = \left[C_D \frac{\ell_o}{D_o}\right]_P \qquad C-36$$

We note first that Eq. C-34 and Eq. C-32 cannot be satisfied simultaneously. Since for gravity dominant horizontal flows it is more important to perserve the effects of gravity which is satisfied by Eq. C-32, then Eq. C-34 indicates that the presure gradient effect will be distorted. For horisontal flow, and in particular for counter current flow, the effect of this distortion should not be serious because the flow of the liquid is determined primarily by gravity and interfacial drag.

The effect of interfacial drag is scaled by Eq. C-36. Experimental data seem to indicate that the drag coefficient depends primarily on the void fraction. Since the requirement of geometric similarity implies the equality of void fractions, these experimental results would imply then the equality of drag coefficients. If this proves to be the case, then Eq. C-36 would reduce to the equality of the ℓ/D ratio between model and prototype. This, in turn, may result in a distortion of the frictional effects given by Eq. C-35 unless the K factors are the same in model and prototype. It is evident that further examination of available data is needed in order to clarify these questions and establish more precisely the rules to scale interfacial drag and wall shear.

C-3 Discussion

To summarize the preceding results. The rules for scaling separated two phase flow (adiabatic and with no mass exchange) using the two fluid model are expressed in terms of two sets of four equations, (one set per phase) plus two coupling equations for momentum exchange at the interface. Assuming geometric similarity, that is, equality of void fractions, Eq. C-26, and of properties, these equations reduce to Eq. C-15 through Eq. C-23. If Eq. C-27 is satisfied, which together with the equality of voids implies equal slip, then one needs to consider only one set, say Eq. C-15 through Eq. C-18, and one coupling equation, say Eq. C-22.

The five other equations pertaining to the other phase are then satisfied automatically.

For separated horizontal gravity dominated flow the requirement to preserve the effects of mass flux, momentum flux, and of gravity, leads to a distortion of time scale given by Eq. C-32 and to a velocity scaling rule given by Eq. C-33. However, the effect of pressure gradient is then distorted. Since the flow of the liquid is determined primarily be gravity and interfacial drag, the effect of this distortion is not serious. Available experimental data need to be examined further in order to establish more precisely the rules for scaling the effects of wall shear and of interfacial drag given by Eq. C-35 and Eq. C-36 respectively.

NRC FORM 335 (7-77)

U.S. NUCLEAR REGULATORY COMMISSION

BIBLIOGRAPHIC DATA SHEET

1. REPORT NUMBER (Assigned by DDC)
NUREG-0724

4. TITLE AND SUBTITLE (Add Volume No., if appropriate)
Problems in Modeling of Small Break LOCA

2. (Leave blank)

3. RECIPIENT'S ACCESSION NO.

7. AUTHOR(S)
Novak Zuber

5. DATE REPORT COMPLETED
MONTH: August YEAR: 1980

9. PERFORMING ORGANIZATION NAME AND MAILING ADDRESS (Include Zip Code)
U.S. Nuclear Regulatory Commission
Division of Reactor Safety Research
Analysis Development Branch
Washington, D. C. 20555

DATE REPORT ISSUED
MONTH: October YEAR: 1980

6. (Leave blank)

8. (Leave blank)

12. SPONSORING ORGANIZATION NAME AND MAILING ADDRESS (Include Zip Code)
U.S. Nuclear Regulatory Commission
Division of Reactor Safety Research
Analysis Development Branch
Washington, D. C. 20555

10. PROJECT/TASK/WORK UNIT NO.

11. CONTRACT NO.
None

13. TYPE OF REPORT
Technical

PERIOD COVERED (Inclusive dates)

15. SUPPLEMENTARY NOTES

14. (Leave blank)

16. ABSTRACT (200 words or less)

The report deals with: (1) two-phase flow regime transitions, (2) liquid entrainment in break flow, (3) vapor pull-through, and (4) CCFL in horizontal ducts.

The first three processes influence the mass flow through the break, whereas the fourth one imposes a limit on liquid flow from the steam generator through the hot leg break into the core.

Correlations available in the literature which deal with these processes are presented and applied to a hot leg of a PWR, LOFT and Semiscale for quantitative estimates, as well as for determining the scale distortion in the latter two facilities.

17. KEY WORDS AND DOCUMENT ANALYSIS

17a. DESCRIPTORS

caling
wo-Phase Flow Regimes
iquid Entrainment in Break
apor Pull Through
CFL in Horizontal Ducts
mall Break Flow Phenomena
orizontal Ducts
Small Break Flow Phenomena
Horizontal Ducts
Applications to PWR, LOFT and Semiscale

17b. IDENTIFIERS/OPEN-ENDED TERMS

18. AVAILABILITY STATEMENT
Unlimited Distribution

19. SECURITY CLASS (This report)
Unclassified

21. NO. OF PAGES

20. SECURITY CLASS (This page)

22. PRICE
$

NRC FORM 335 (7-77)